IL
NUOVO CIMENTO
ORGANO DELLA SOCIETÀ ITALIANA DI FISICA
SOTTO GLI AUSPICI DEL CONSIGLIO NAZIONALE DELLE RICERCHE

VOL. VIII, N. 10 *Serie nona* 1 Ottobre 1951

An intrinsic angular analysis of cosmic ray stars.

M. DELLA CORTE and M. GIOVANNOZZI
Istituto di Fisica dell'Università - Firenze

(ricevuto il 14 Luglio 1951)

Summary. — An intrinsic analysis of three-pronged stars has been carried out. From the distribution of « resultants », « apertures » and « volumes », it appears reasonable to assume that a certain number of « recoils » are due to a fission-like process. For low-energy stars, there is some experimental evidence of the complete disintegration of light nuclei.

Cosmic ray stars which had been produced in Ilford G.5 plates, have been studied in order to investigate the intrinsic angular distribution of prongs in each star. The plates had been exposed at the Testa Grigia Laboratory (3 500 m a.s.l.).

We report here the preliminary results of this analysis for three-pronged stars. Tracks whose length exceeded 5 μ were considered as « prongs », while those of minor length were classified as « recoils ». At present our statistics are not rich enough to warrant a complete energetic analysis. Tracks were simply classified as « black », when their grain density was more than about 150 grain/100 μ; while all the others, including a few relativistic particles, were classified as « gray ».

The analysis was carried out as follows:

1) A unit vector was ascribed to the projection of each prong on the plane of the emulsion; the distribution of their resultants, both in modulus

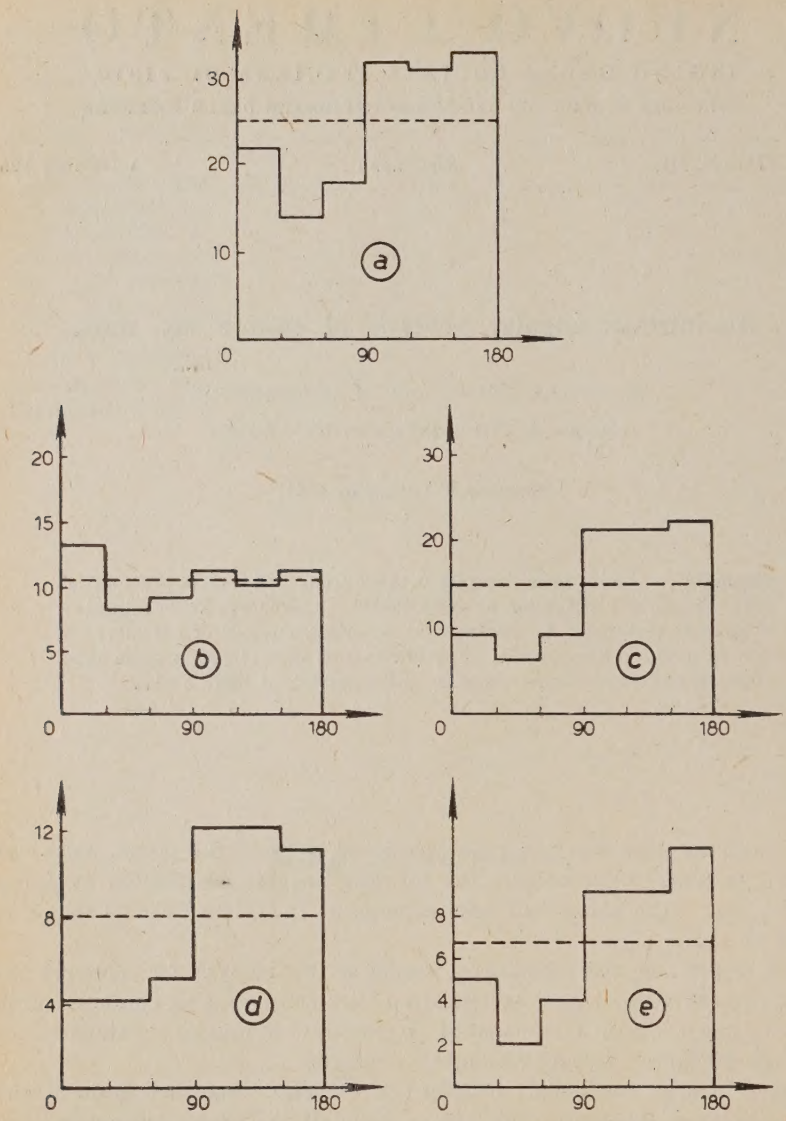

Fig. 1. – Angular distribution of resultants with respect to the vertical. *a*) All the three-pronged stars. *b*) Stars with recoil. *c*) Stars without recoil. *d*) Stars without recoil and all prongs « black ». *e*) Stars without recoil and at least one « gray » prong. Dotted lines represent and isotropical distribution.

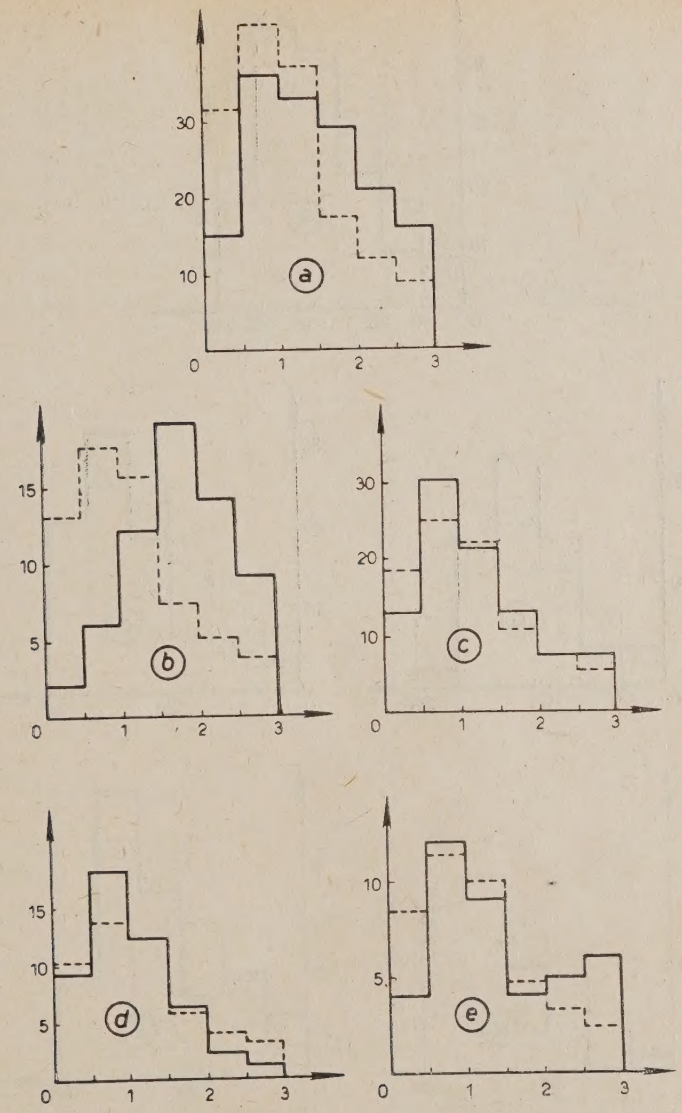

Fig. 2. – Distribution in modulus of the resultants. *a*) All the stars. *b*) Stars with recoil. *c*) Stars without recoil. *d*) Stars without recoil and all prongs « black ». *e*) Stars without recoil and at least one « gray » prong. Dotted lines represent the « Random Walk » distribution.

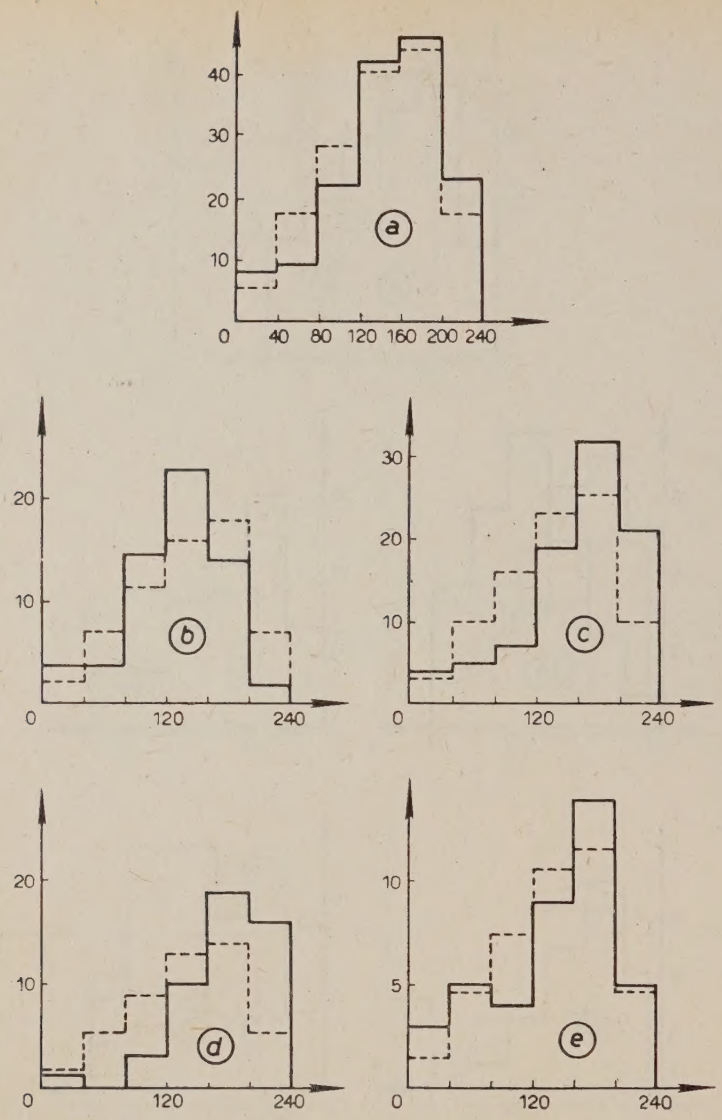

Fig. 3. – Distribution of the aperture of the stars. *a*) All the stars. *b*) Stars with recoil. *c*) Stars without recoil. *d*) Stars without recoil and all prongs « black ». *e*) Stars without recoil and at least one « gray » prong. Dotted lines represent an isotropical distribution.

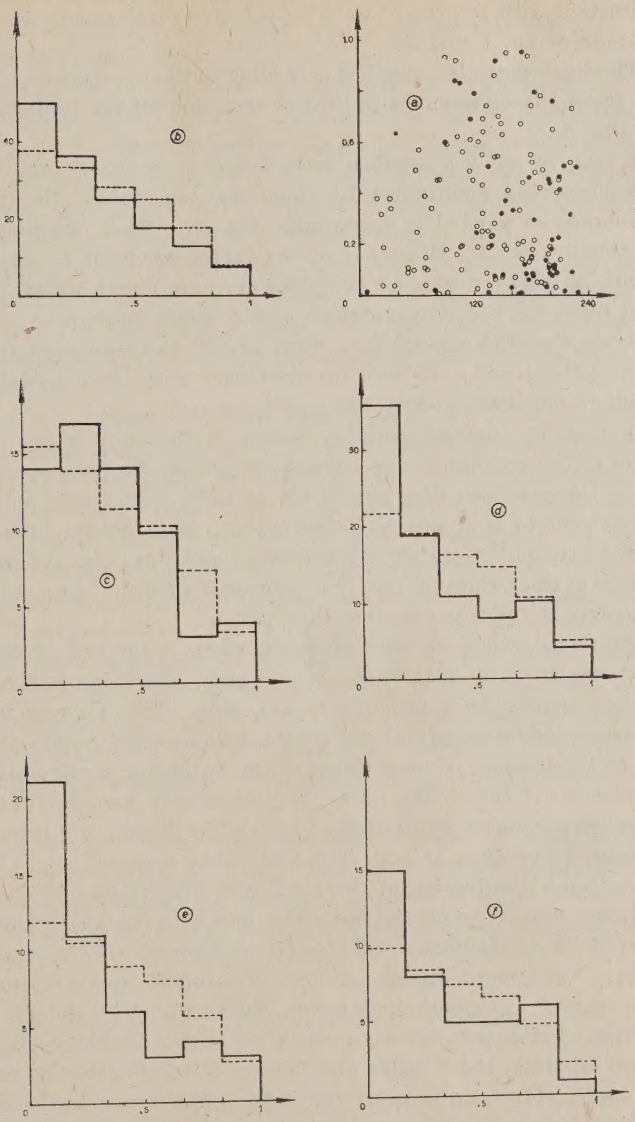

Fig. 4. – Distribution of the volumes of the stars. *a*) All the stars. *b*) Correlation between apertures and volumes: (•) Stars without recoil and all the prongs « black ». (○) All the other stars. *c*) Stars with recoil. *d*) Stars without recoil. *e*) Stars without recoil and all prongs « black ». *f*) Stars without recoil and at least one « gray » prong. Dotted lines represent an isotropical distribution.

and in direction with respect to the vertical, was investigated and is plotted in histograms of fig. 1 and 2.

2) The stars were also classified according to their « aperture »; by « aperture » we mean the minimum angle which contains all the projections of the 3 prongs (fig. 3).

3) A unit vector was ascribed to each prong (in space) and the volume of the parallelepiped determined by them was calculated; the distribution of such volumes is plotted in histograms (fig. 4). Such distribution, while much simpler to evaluate than that of the vector resultant in space ([1]), supplies us with an easy criterion for complanarity, and might afford, as we shall see, useful hints for the interpretation of the whole picture.

The above statistics extend to a total of 150 three-pronged stars, 62 of which were with « recoil »; 48 with no recoil and with three « black » prongs, and 40 with no recoil and at least one « gray » prong.

The methods of analysis adopted, except in the case of the directional distribution of the resultants, are intrinsic in nature, i.e. do not involve any reference to the supposed direction of the primary. Full lines in the histograms correspond to the observed distribution, while dotted lines represent the expected distribution on the hypothesis of isotropy; e.g. the distribution of the moduli of the resultants (fig. 2) is compared with the expected « random walk » distribution for three vectors in a plane.

Histogram 2 *a*), which includes all stars, shows a marked excess of large resultants, over the « random walk » expectation, which appears to indicate an association among the prongs of the same star. Two different hypotheses offer themselves spontaneously to explain this experimental result: *a*) a « drag » effect due to the transfer of momentum of the impinging particle on the evaporating nucleus; if this is the case, the evaporated particles must appear to be projected preferably downwards; *b*) the effect is due to a peculiar mode of production of the star, as, e.g. in a fission-like process.

The directional distribution of the resultants with respect to the vertical, shows a definite preference for the downward direction (fig. 1 *a*)) which has also been observed by A. MANFREDINI ([2]) for the distribution of the single prongs of the stars. This would appear, at first, to support interpretation *a*).

A more careful examination, however, shows (fig. 2 *b*) and *c*)) that the excess of large resultants is mainly due to stars with a visible recoil; now just for this class of stars, the angular distribution of resultants does not appear to depart appreciably from isotropy (fig. 1 *b*)). This latter result leads us to believe that an effect of the type *b*) plays a prominent role.

([1]) D. H. PERKINS: *Nature*, **161**, 486 (1948).

([2]) A. MANFREDINI: *Nuovo Cimento*, **7**, 195 (1951).

We could namely suppose that a certain number of recoils are due to a fission followed by the evaporation of one of the fragments, the other then appearing as a recoil track.

An hypothesis of this kind has already been put forward by HARDING, LATTIMORE and PERKINS [3] to explain some remarkable features observed by them in stars with numerous prongs (> 7). This does not exclude, however, that recoils may also consist of residual fragments of the nucleus which, by a statistical fluctuation in the distribution of evaporated particles, happen to get a sufficient momentum to become visible tracks.

According to A. MANFREDINI, stars with recoil are most likely due to disintegrations of heavy nuclei; this is confirmed by fig. 1 *b*) and *c*) which clearly show the absence of a drag effect for such type of stars. It follows that a noticeable percent of the stars with no recoil represents disintegrations of light nuclei.

Let us now consider the stars with no recoil and all three prongs « black »; such low-energy stars show (fig. 3 *d*)) an excess of large apertures with respect to the expected isotropical distribution, while their volume distribution shows an excess of small volumes, that is, a definite trend towards complanarity of prongs. It is also noteworthy, that for these low-energy stars there is a strong correlation between small volumes and large apertures. Since there is no strict « a priori » correlation between apertures and volumes (fig. 4 *b*)) (and, in fact, this is observed only in low-energy stars), the experimental evidence reported above suggests that a considerable number of low energy stars represent the complete evaporation of a light nucleus, the whole set of particles which contribute to momentum balance thus showing up as ionizing tracks. Further measurement are now under way, in view of enriching our statistics and to test the suggested interpretation of the experimental results.

We whish to express our appreciation to Prof. S. FRANCHETTI, Director of this Institute, Prof. M. MANDÒ, and to Dr. T. FAZZINI for their valuable suggestions and helpful discussions in connection with this work. Thanks are also due to Miss M. RAMAT for her help in analysing the photographic plates.

---

[3] J. B. HARDING, S. LATTIMORE and D. H. PERKINS: *Proc. Roy. Soc.*, **106**, 325 (1949).

RIASSUNTO

È stata eseguita una analisi angolare intrinseca (cioè indipendente dalla direzione del primario) su 150 stelle a tre rami. Dalla distribuzione delle risultanti delle proiezioni dei singoli rami nel piano dell'emulsione, e dalle distribuzioni delle « aperture » e dei « volumi » delle singole stelle si mettono in evidenza delle anomalie rispetto a quanto prevedibile per una emissione isotropa delle particelle. L'esperienza sembra suggerire che i « recoils » sono da attribuire, almeno in parte, ad un processo di fissione. La marcata tendenza alla complanarità dei rami delle stelle di piccola energia viene interpretata con la presenza di un numero sensibile di disintegrazioni complete in nuclei leggeri dell'emulsione.

IL NUOVO CIMENTO Vol. VIII, N. 10 1 Ottobre 1951

On the Universal Fermi-Type Interaction (II).

E. R. Caianiello

University of Rochester - Rochester, N.Y., U.S.A.

(ricevuto il 17 Luglio 1951)

Summary. — We search for a universal interaction among all known fermions based on invariance under the extended Lorentz group which will exclude all processes not occurring in nature. Two mutually exclusive interactions appear ultimately to be the only ones consistent with certain plausible criteria of simplicity. The two possible interactions are proved to yield identical numerical answers in the case of free fermions; one at least of them is in excellent agreement with all the experimental evidence available thus far.

1. – Introduction.

In a previous work [1], referred to hereafter as I, it has been proved that it is possible to meet the requirements for a universal Fermi interaction (that is, a direct interaction with a unique coupling constant among any four of the five particles of spin $1/2\hbar$ — neutrino (ν), electron (e), μ-meson (μ), proton (P), neutron (N) — and their anti-particles such that processes not observed in nature are ruled out by charge conservation and Lorentz invariance), provided some qualitative assumptions are made regarding the types of the particles and the structure of the interaction. That is, out of the 16^5 a priori possible type assignments only those should be selected which require, for overall invariance, that the coefficients of the spinor products appearing in the Hamiltonian density transform like a tensor density. In order to give

[1] E. R. Caianiello: *Nuovo Cimento*, **7**, 534 (1951).

concreteness to the treatment, use was made of a particular type of interaction, obtained by a formal modification of the Wigner-Critchfield interaction; it was, however, emphasized that, in the author's opinion, there was no ground for claiming the physical correctness of that choice.

It was furthermore proved that, if a universal interaction should obtain solely from arguments of charge conservation and relativistic invariance, besides the experimentally observed processes

$$(1) \qquad \begin{cases} N \to P + e + \nu \\ \mu \to e + 2\nu \\ \mu^- + P \to N + \nu , \end{cases}$$

the only other processes which need to be regarded as occurring in nature are:

$$(II) \qquad \begin{cases} P + \bar{P} \to 2\nu \\ N + \bar{N} \to 2\nu \\ \mu + \bar{\mu} \to 2\nu \\ e + \bar{e} \to 2\nu \\ \nu + \bar{\nu} \to 2\nu , \end{cases}$$

(and their charge conjugates; the bar denotes antiparticle). Such processes as scattering of fermions by fermions, which have been previously included in the general scheme of a β-decay interaction ([2]), are excluded and would appear, therefore, to be of a different nature.

Since I was completed, experimental results ([3]) have been published on the decay of the μ-meson. They support the view that two mass zero particles are emitted, and exhibit a spectrum which has zero intensity for maximum energy of the emitted electron, within experimental error. The last feature is of particular importance, since it sets rather stringent requirements on the theory used to describe this decay; in particular, it rules out the Wigner-Critchfield interaction, which yields a non-vanishing end point.

This circumstance has led us to a re-examination of the whole subject, the results of which are presented in this paper. We consider here first the most general interaction compatible with the qualitative requirements shown in I to be necessary for the exclusion of the unwanted processes; then, by applying some plausible criteria of simplicity, we restrict the universal interaction to two *mutually exclusive* possible interactions, one of which at least results in excellent agreement with all the evidence available thus far, although

---

([2]) L. MICHEL: *Proc. Phys. Soc.*, **63A**, 514 (1950).

([3]) SAGANE, GARDNER and HUBBARD: *Phys. Rev.*, **82**, 557 (1951).

the two interactions will be proved to yield identical numerical answers in any physical process involving free particles.

Hence, the task of selecting between the two interactions on theoretical grounds will require a different approach, such as the determination, if possible, of the actual types of the fermions. Perhaps, this can be done by considering all reactions among fermions — and of them with bosons — other than β-decay. Such a study will presumably have a bearing on questions of parity for mesons; it is considered to lie beyond the scope of this work, which only attempts to determine the universal interaction once its possibility has been recognized.

In Part **2**, we prove the intrinsic nature of the fermion types, by showing them to be independent of the representation used for the Dirac matrices, and state our notations.

Part **3** describes the method by which we arrive at the actual determination of the universal interaction. In Parts **2** and **3**, we give a more thorough treatment of some questions which were only sketched in the preceding work.

Finally, Part **4** examines the physical predictions resulting from the theory.

2. – Space and time inversions, charge conjugation and fermion types.

We consider here, in a more exhaustive manner, some of the questions already treated in I. We prove that the types of the fermions under space and time inversions are independent of the representation in which the Dirac equation is formulated — a necessary requirement, if they are to be regarded as intrinsic properties of the elementary particles to which they are attached.

If S, V, T are respectively a scalar, vector or tensor quantity, we denote with S' (instead of PS), V', T', the corresponding pseudoquantities. If a quantity transforms like a vector under space inversion I_S and like a pseudovector under time inversion I_T, we say that it is a (V_S, V'_T); likewise in similar cases.

In an arbitrary representation of the Dirac matrices, I_S, I_T and the charge-conujgation operator I_C are given respectively (as is well known [4]; see also I) by:

$$I_S = \varrho_S \gamma^4 ; \qquad I_T = \varrho_T u_T K ; \qquad I_C = u_C K .$$

K is the complex-conjugation operator; ϱ has one of the values $+1$, -1,

---

[4] See for instance: E. WIGNER: *Nach. Ges. Wiss., Göttingen*, 546 (1932) and W. PAULI: *Ann. Inst. H. Poincaré*, **6**, 109 (1936). The statement made about ϱ_T is justified later in this Part.

$i, -i$ which determines the type A, B, C, D of the fermion (we have taken $\varrho_C = +1$). The form of I_T is a consequence of the assumption that the time-inversion operator must reverse the trajectory of the particle, but not its charge, and of the fact that the electromagnetic four-vector A^μ is a (V_S, V'_T), (as follows immediately from the Maxwell equations or from the expression of the relativistic four-momentum). The matrices u_T and u_C satisfy the relations

$$(1) \qquad u_T \bar{\gamma}^\mu u_T^{-1} = \gamma^\mu \; ; \qquad u_C \bar{\gamma}^m u_C^{-1} = \gamma^m \; ; \qquad u_C \bar{\gamma}^4 u_C^{-1} = -\gamma^4 \, ,$$

($^-$ denotes complex conjugate; * and $\tilde{}$ will denote transpose and charge conjugate respectively). If ψ is of type ϱ_T, the type under I_T of its charge conjugate $\tilde{\psi} = u_C \bar{\psi}$ can be determined from:

$$(2) \qquad \tilde{\psi}' = u_C \bar{\psi}' = \bar{\varrho}_T u_C \bar{u}_T \psi = \bar{\varrho}_T u_T \bar{u}_C \psi = \bar{\varrho}_T u_T K \tilde{\psi} \, .$$

The last equalities follow formally from (1): those equations imply indeed that both $u_C \bar{u}_T = S_1$ and $u_T \bar{u}_C = S_2$ satisfy the relations

$$S\gamma^m = \gamma^m S \; ; \qquad S\gamma^4 = -\gamma^4 S \; ;$$

we can take then

$$S_1 = \gamma^1 \gamma^2 \gamma^3 \; ; \qquad S_2 = \alpha S_1 \, ,$$

α being a constant whose value is given by:

$$\alpha = S_1^{-1} u_T S_1 u_T^{-1} = S_1^{-1} u_T \bar{\gamma}^1 \bar{\gamma}^2 \bar{\gamma}^3 u_T^{-1} = S_1^{-1} S_1 = 1 \, ,$$

again because of (1), and since

$$u_C = \alpha u_T^{-1} S_1 = \bar{S}_1 u_T^{-1} \, .$$

The equalities

$$u_C \bar{u}_T = u_T \bar{u}_C = \gamma^1 \gamma^2 \gamma^3$$

are also clear from a physical point of view, since $I_T I_C$ and $I_C I_T$ must each coincide with some determination of the time inversion operator $\varrho_T \gamma^1 \gamma^2 \gamma^3$ defined by PAULI, that reverses also the charge of the particle. In particular, this observation enables us to restrict the phase factor in I_T — which otherwise would be arbitrary — to one of the values of ϱ_T, once ϱ_C has been taken $= +1$. It appears from (2) that if the type of ψ under I_T is ϱ_T, that of $\tilde{\psi}$ is $\bar{\varrho}_T$, regardless of the representation used. It also clearly follows from (1) that the type of $\tilde{\psi}$ under I_S is given by $-\bar{\varrho}_S$, in any representation.

Being thus assured that our treatment is not impaired by any loss of rigor

or generality, we adhere in the following strictly to the Majorana representation of the Dirac matrices (5), which presents remarkable advantages of formal simplicity. In this representation:

$$\gamma^\mu\gamma^\nu + \gamma^\nu\gamma^\mu = 2\delta_{\mu\nu}\,; \qquad \bar{\gamma}^{\mu *} = \gamma^\mu\,,$$

$$\gamma^k = \gamma^{*k} = \bar{\gamma}^k; \qquad \gamma^4 = -\bar{\gamma}^4 = -\gamma^{4*}\,, \tag{4}$$

$$u_C = 1\,; \quad I_C = K\,; \quad I_S = \varrho_S\gamma^4\,, \quad I_T = \varrho_T\gamma^1\gamma^2\gamma^3 K. \tag{5}$$

3. – Determination of the universal interaction.

3·1. – As was done already by YANG and TIOMNO and in I, we consider the field of a particle and of its charge conjugate as different entities; we write accordingly the most general Hamiltonian density for the interaction among any four fermions a, b, c, d as

$$H = A_{\alpha\beta\gamma\delta}\psi_\alpha^{(a)}\psi_\beta^{(b)}\psi_\gamma^{(c)}\psi_\delta^{(d)} + \text{Herm. Conj.}\ (6)\,, \tag{6}$$

(summation convention), it being understood that $\psi^{(\bar{a})} = \bar{\psi}^{(a)}$. The customary treatment of the β-decay theory, where the types of the fermions are not taken into account, assumes that the coefficients $A_{\alpha\beta\gamma\delta}$ of the spinor products are (S_S, S_T). It has been shown in some detail in I that, while this assumption does not lead to the exclusion of all of the unwanted processes, the other assumption $((S'_S, S'_T)$ does, as it requires that also the $\psi_\alpha^{(a)}\psi_\beta^{(b)}\psi_\gamma^{(c)}\psi_\delta^{(d)}$ are (S'_S, S'_T) and leads therefore to appropriate choices for the types under I_S and I_T of ν, e, μ, P, N which fulfill the requirements for a universal interaction. The processes (II) already mentioned in the Introduction accompany then *necessarily* the processes (I). While we refer to I for the proof of this fact, which we shall find of decisive importance in the actual determination of the universal interaction, we think it useful to report in the Appendix *all* the type assignments for ν, e, μ, P, N (672 out of 16^5) that are compatible with the hypothesis (S'_S, S'_T). If the idea of a universal interaction proves to be correct, such knowledge will be the indispensable starting point for the precise determination of the actual types of the five fermions involved. It should be noted that some arbitrariness is still left in the assignments reported in

(5) E. MAJORANA: *Nuovo Cimento*, **14**, 171 (1937). See also Note (2). In I, use has been made of the Pauli representation.

(6) C. YANG and J. TIOMNO: *Phys. Rev.*, **79**, 495 (1950). See also: A. GAMBA: *Nuovo Cimento*, **7**, 919 (1950).

Table I (see Appendix); one could, for instance, obtain, with only slight changes, instead of processes (II) the processes

$$\text{(II')} \qquad \begin{cases} P + \bar{P} \to \nu + \bar{\nu} \\ N + \bar{N} \to \nu + \bar{\nu} \\ \mu + \bar{\mu} \to \nu + \bar{\nu} \\ e + \bar{e} \to \nu + \bar{\nu} \\ \nu + \bar{\nu} \to \nu + \nu \ (\text{or } \bar{\nu} + \bar{\nu}) \end{cases}$$

To this, we add the remark that it is possible to obtain processes (I) and (II) — and only them — also with the prescription (S'_S, S_T). Table II reports all the corresponding types. It will be apparent from the following that there exists no interaction consistent with the choice (S_S, S'_T), which, otherwise, would be equally satisfactory.

Tables I and II correspond to the « normalizations »

$$N + \nu \to P + e\,; \qquad \mu^- + P \to N + \nu\,; \qquad \mu + \bar{e} \to \nu + \nu \ (\text{or: } \bar{\nu} + \bar{\nu})\,,$$

for processes (I), besides those already exhibited by processes (II)). Changes are possible, as already said; their study is beyond our scope, and belongs rather to the determination of the actual types of the physical particles, mentioned in the Introduction. All we need to know, here, is that only the two mutually exclusive hypotheses (S'_S, S'_T) and (S'_S, S_T) can yield an interaction of the desired character.

We shall term the coupling corresponding to these hypotheses « odd », reserving the name « even » for those of the customary theory (S_S, S_T). Odd couplings have been considered explicitly for the first time in ref. [5].

3·2. – In the following, we shall use throughout the language and formalism of the c-number theory. This will only simplify our formal developments: the transcription into the q-theory is self-evident, and we have nothing to add in this respect to the excellent treatment given by MICHEL [2]. The chief differences would be the necessity of speaking there of symmetrization instead of antisymmetrization (since the use of field operators already implies the exclusion principle) and the opportunity of using one of the several devices described in ref. [2] which makes all of the fields anticommute, whether corresponding to identical particles or not.

We write the 16 matrices γ^A of the Dirac algebra as

$$\text{(8)} \qquad \begin{cases} 1 \\ \gamma^\mu \\ \gamma^{[\mu\nu]} = i\gamma^4\gamma^k\gamma^5\,; \quad i\gamma^k\gamma^4 \\ \gamma^{[\lambda\mu\nu]} = i\gamma^\mu\gamma^5 \\ \gamma^5 = \gamma^1\gamma^2\gamma^3\gamma^4\,. \end{cases}$$

Then, as is well known:

$$\gamma^{A^2} = 1 , \qquad \gamma^{A*} = \gamma^A ;$$

$$\sum_{A=1}^{16} \gamma^A_{\alpha\beta}\gamma^A_{\gamma\delta} = 4\delta_{\beta\gamma}\delta_{\alpha\delta} ,$$

$$\sum_{A=1}^{16} \sum_{\varrho,\sigma=1}^{4} \gamma^A_{\beta\gamma}\gamma^B_{\alpha\varrho}\gamma^A_{\varrho\sigma}\gamma^{B'}_{\sigma\delta} = 4\gamma^B_{\alpha\gamma}\gamma^{B'}_{\beta\delta} .$$

Since the 16×16 Kronecker products $\gamma^A\times\gamma^B$ form a complete basis for the complex algebra of the 16×16 matrices, the interaction (6) reduces to a sum of terms

$$(10) \qquad H = \sum_{A,B} \sum_{P} g_{A,B,P}(\gamma^A\times\gamma^B)_{\alpha\beta,\gamma\delta}\psi^{(\bar a)}_\alpha\psi^{(\bar b)}_\beta\psi^{(c)}_\gamma\psi^{(d)}_\delta + \text{Herm. Conj.}$$

$$= \sum_{A,B} \sum_{P} g_{A,B,P}(\tilde\psi^{(a)*}\gamma^A\psi^{(c)})(\tilde\psi^{(b)*}\gamma^B\psi^{(d)}) + \text{H.C.}$$

the $g_{A,B,P}$ playing the role of coupling constants, the index P denoting the permutations of the four particles cd, ab (7). We shall write a typical term of (10), more simply, as:

$$(11) \qquad \langle a\gamma^A c\rangle\langle b\gamma^B d\rangle .$$

This is, of course, the customary treatment, which leads in the case of even couplings to the well known five invariant interactions of the β-decay theory. It is to be explicitly noted that — as shown in ref. (8) and (2), and even more comprehensively in a very recent treatment due to Mac-Callum and Wightman (9) — once a « pure » interaction has been selected out of the five, the order in which the permutation of the four particles is fixed is of actual physical significance, since a re-ordering of the particles would change that interaction into some linear combination of all five. This is of basic importance for our purposes, and we shall consider in the following the order exhibited by (11) as the « normal order », in which c, d and a, b play the role, respectively, of initial and final particles, and $c\to a$, $d\to b$.

From (8) one forms the matrices

$$(12) \qquad \begin{cases} S = \gamma^4 & S' = S\cdot(i\gamma^5) \\ V^\mu = i\gamma^4\gamma^k\ ;\ 1 & V'^\mu = V^\mu\cdot(\gamma^5) \\ T^\mu = i\gamma^k\gamma^5\ ;\ \gamma^k & T'^\mu = T^\mu\cdot(-i\gamma^5) , \end{cases}$$

(7) Note that we write now, for convenience $\bar a$, $\bar b$ instead of a, b.

(8) M. Fierz: *Zeits. für Phys.*, **104**, 553 (1937).

(9) C. J. MacCallum and A. S. Wightman: *Princeton University, Technical Report NOL* No. 7 (1951).

which inserted between $\tilde{\psi}^*\psi$ yield the well known transformation laws under Lorentz rotations. The appearance of T'^{μ} is typical of the odd couplings. We have now to investigate which « pure » couplings are allowed by each of the hypotheses (S'_S, S'_T), (S'_S, S_T), (S_S, S'_T), which only may yield a universal interaction as discussed in the previous section. It is obvious that no terms of type $(a\gamma^A c)(b\gamma^A d)$ can appear, as they would correspond to the hypothesis (S_S, S_T), and that we must combine terms having the same transformation properties with respect to rotations. We are left therefore with the possibilities (when the order of the particles is not explicitly exhibited, we shall understand it to be the normal order, which we denote by writing $J(cd/ab)$):

$$
(13)\qquad \begin{cases}
J = \langle a\gamma^4 c\rangle\langle bi\gamma^4\gamma^5 d\rangle & + \text{ Herm. Conj.} \\
J' = \langle ai\gamma^4\gamma^5 c\rangle\langle b\gamma^4 d\rangle & + \quad » \\
J'' = \langle ai\gamma^k\gamma^5 c\rangle\langle b\gamma^k d\rangle + \langle a\gamma^k c\rangle\langle bi\gamma^k\gamma^5 d\rangle & + \quad » \\
J_1 = \langle ai\gamma^4\gamma^k c\rangle\langle bi\gamma^k\gamma^4\gamma^5 d\rangle - \langle a1c\rangle\langle b\gamma^5 d\rangle & + \quad » \\
J'_1 = \langle ai\gamma^4\gamma^k\gamma^5 c\rangle\langle bi\gamma^4\gamma^k d\rangle - \langle a\gamma^5 c\rangle\langle b1d\rangle & + \quad »
\end{cases}
$$

By applying I_S and I_T to these J's, we obtain a product of ϱ and $\bar{\varrho}$ which is ± 1, and correspondingly, in accord with the requirements of overall invariance, $\pm J$ from the action of γ^4 and $\gamma^1\gamma^2\gamma^3$ on the matrices inside. (I_T requires, of course, a transposition which has the effect of changing a term into its Hermitean conjugate). The result is that J, J' and J'' fit the hypothesis $(S'_S\, S'_T)$ and are also invariant under charge conjugation; J_1 and J'_1 fit the hypothesis (S'_S, S_T) and change their sign under charge conjugation. This last feature, however, is not by itself sufficient to discard J_1 and J'_1, since the prescription $\varrho_C = +1$ for all the fermions is arbitrary, and might be modified by specific assignments of ϱ_C for each particle. In this case J, J', J'' would not be invariant under I_C; we can therefore regard this only as a further argument to assert that the couplings J, J', J'' and J_1, J'_1 are mutually exclusive, and correspond respectively to the hypotheses (S'_S, S'_T) and (S'_S, S_T). Obviously no coupling satisfies (S_S, S'_T).

It is well to remark explicitly that if a J corresponds to the hypothesis (S'_S, S'_T), iJ corresponds to the hypothesis (S'_S, S_T), and conversely, since I_T and I_C contain the complex conjugation operator K. This circumstance will have a bearing on the discussion in the next section, and clearly implies that all of the five interactions (13) can occur together in a linear combination, in either hypothesis, if some of the coupling constants are allowed to be imaginary.

3·3. – In order to achieve our aim, we have first to investigate the behavior of the pure interactions J, J', J'', J_1, J'_1 under permutations of the particles, and then look for some plausible criteria of simplicity. In doing so, however, we shall discuss all the cases that may occur, since some interaction other

than the ones here finally chosen may eventually turn out to have physical interest. One of these criteria, which we have already been using implicitly, is that of restricting the coupling constants to real values.

Let (ab) denote the transposition of the particles a and b. Since any permutation of the symmetric group of four elements $abcd$ can be reduced to a product of transpositions, it will be sufficient to investigate the effect on the J's of the six possible transpositions. Actually, any four of these constitute a complete set of generators of the group, e.g. $(ad)=(ac)(cd)(ac)$, $(bc)=(bd)(cd)(bd)$; for completeness we give explicitly the matrix form of all six. This follows by considering them as acting on a five-vector $\boldsymbol{J}=(J, J', J''; J_1, J_1')$ and by using the relations (4) and (9) [8]. One finds, if $J(cd/ba)=(ab)J(cd/ab)$, etc., that the six transpositions are represented in the vector space spanned by $\boldsymbol{J}$ by the matrices:

$$(ac)=\begin{pmatrix} -1 & & & & \\ & -1 & & 0 & \\ & & 1 & & \\ & 0 & & 1 & \\ & & & & -1 \end{pmatrix}; \qquad (bd)=\begin{pmatrix} -1 & & & & \\ & -1 & & 0 & \\ & & 1 & & \\ & 0 & & -1 & \\ & & & & 1 \end{pmatrix}$$

$$(ad)=\begin{pmatrix} 1/4 & 1/4 & 1/4 & -i/4 & -i/4 \\ 1/4 & 1/4 & 1/4 & i/4 & i/4 \\ 3/2 & 3/2 & -1/2 & 0 & 0 \\ i & -i & 0 & -1/2 & 1/2 \\ i & -i & 0 & 1/2 & -1/2 \end{pmatrix}; \qquad (ab)=\begin{pmatrix} 1/4 & 1/4 & -1/4 & -i/4 & i/4 \\ 1/4 & 1/4 & -1/4 & i/4 & -i/4 \\ -3/2 & -3/2 & -1/2 & 0 & 0 \\ i & -i & 0 & -1/2 & -1/2 \\ -i & i & 0 & -1/2 & -1/2 \end{pmatrix}$$

$$(bc)=(\overline{ad}); \qquad (cd)=(\overline{ab}).$$

It is clear that the most general odd interaction is a linear combination of the five pure interactions (13), the coupling constants being imaginary where needed for each term in it to have the same transformation properties under time inversion and charge conjugation.

Possible Forms of the Universal Interaction.

3·4. – The criteria adopted will be elucidated with a view to rendering them as plausible as possible. It should, however, be understood that ultimately they are only postulates, whose correctness may only be inferred a posteriori from adherence to physical reality. The fundamental idea is that the universal interaction, if it exists at all, should exhibit marked features of symmetry and simplicity. The interactions corresponding to even couplings are invariant under the substitution $(ab)(cd)$; of the interactions (13), only J''

has this property; J, J' and J_1, J_1' are interchanged by $(ab)(cd)$. One would expect therefore J, J' and J_1, J_1' to appear in a completely symmetric manner.

Furthermore, some of the processes (I) and (II) imply the appearance of identical particles either in *final* or *initial* states. It was indeed remarked that a slight change of type assignments would lead from processes (II) to processes (II′): but in any case the reactions

$$\nu + \bar{\nu} \to \nu + \nu ,$$

and

$$\nu + \nu \to \nu + \bar{\nu} ,$$

will always exhibit the same form. It is certainly consistent with the idea of maximum simplicity to ask that the interaction be of such a nature that all particles are treated by it in a like manner, whether identical or not, so that no further procedures of antisymmetrization should be required for particular processes. We shall find that the requirement of antisymmetrization on *both* the initial particles c, d and the final a, b is indeed the one that gives the most satisfactory result from the point of view of both uniqueness and simplicity. To prove this, we must first consider all the possible antisymmetrizations, i.e. on any two, three, two-two and four particles. The corresponding operators that act on the five-vector $\boldsymbol{J}$ are given by

$$(15)\quad \begin{cases} \mathcal{A}(ab) = [1 - (ab)] \\ \mathcal{A}(abc) = [1 + (abc) + (acb)][1 - (ac)] \\ \mathcal{A}(cd/ab) = [1 - (ab)][1 - (cd)] = \mathcal{A} \\ \mathcal{A}(abcd) = [1 - (ac) - (bd) - (ad) - (bc) + (ac)(bd)] \cdot [1 - (ab)][1 - (cd)] \end{cases}$$

and by those resulting from them by change of the letters; the explicit expressions follow from (14). We have omitted the numerical coefficients necessary to make them idempotent (1/2, 1/6, 1/4, 1/24) since ultimately we shall choose one of them, and the corresponding coefficient can be thought of as incorporated in the coupling constant. The first three operators listed in (15) are seen on simple inspection to be actually antisymmetrization operators; the fourth can be shown by direct computation to be only a more convenient expression of the customary one:

$$\mathcal{A}(abcd) = C_1 - C_2 + C_3 + C_4 - C_5 ,$$

where

$$(+, 1)C_1 = 1 ; \quad (-, 6)C_2 = (ab) ; \quad (-, 8)C_3 = (abc) ;$$

$$(+, 3)C_4 = (ab)(cd) ; \quad (-, 6)C_5 = (abcd) ,$$

are the conjugate classes of the symmetric group on four elements, with the

parity and number of elements of each shown in the brackets. We have already pointed out before that, once a pure interaction is prefixed, the order in which the particles appear in it has a concrete physical meaning. To apply therefore $\mathcal{A}(ac)$ to a $J(cd/ad)$ would now mean to antisymmetrize in two particles, one of which is initial and the other final: this is not a physical requirement (the explicit expressions derive immediately from (14) — the results would not be unique, and would disagree with experiment). On the contrary, $\mathcal{A}(ab)$ and $\mathcal{A}(cd)$ correspond to actual cases; it can be seen from (14) that they lead to a linear combination of the $J(cd/ab)$'s with imaginary constants. Of the operators that antisymmetrize three particles, we consider only the expressions of $\mathcal{A}(abc)$:

$$\mathcal{A}(abc) = \begin{pmatrix} 1 & -1 & 0 & 0 & -i \\ -1 & 1 & 0 & 0 & i \\ 0 & 0 & 0 & 0 & 0 \\ 0 & 0 & 0 & 0 & 0 \\ 4i & -4i & 0 & 0 & 4 \end{pmatrix}.$$

This combines $J(cd/ab)$, $J'(cd/ab)$ and $J_1'(cd/ab)$, again with imaginary constants.

$\mathcal{A}(abcd)$ turns out to vanish identically. This shows that there is no interaction completely antisymmetric in all four particles if we use odd couplings: in agreement with the well known fact that the only completely antisymmetric combination of four spinors is given by the Wigner-Critchfield interaction, and contrary to the interaction used in I (which is perfectly sound if one takes the view that the constant g appearing in it is by itself an (S_S', S_T') — there is no objection in principle against this except one of simplicity). We are left with $\mathcal{A}(cd/ab)$:

$$\mathcal{A} = \mathcal{A}(cd/ab) = \begin{pmatrix} 1/2 & 1/2 & 1/2 & 0 & 0 \\ 1/2 & 1/2 & 1/2 & 0 & 0 \\ 3 & 3 & 3 & 0 & 0 \\ 0 & 0 & 0 & 2 & 2 \\ 0 & 0 & 0 & 2 & 2 \end{pmatrix}.$$

It yields:

$$(16) \quad \mathcal{A}J(cd/ab) = \mathcal{A}J'(cd/ab) = \frac{1}{6}\mathcal{A}J''(cd/ab) =$$

$$= \frac{1}{2}J(cd/ab) + \frac{1}{2}J'(cd/ab) + \frac{1}{2}J''(cd/ab),$$

and

$$(17) \quad \mathcal{A}J_1(cd/ab) = \mathcal{A}J_1'(cd/ab) = 2J_1(cd/ab) + 2J_1'(cd/ab).$$

Apart from a different normalization of the coupling constant, if one starts from the pure odd tensor coupling (the necessity of which has already been pointed out several times in the literature [9], [10]), we see that this is the only procedure of antisymmetrization which does not introduce imaginary coupling constants and which determines uniquely the universal interaction for either hypothesis (S'_S, S'_T) or (S'_S, S_T). (If, on the other hand, one is willing to accept imaginary coupling constants, or not willing to follow this line of thought, the arbitrariness is of course much larger).

The choice of two particles as initial and the remaining two as final leads actually to three possible modes of decay: $c + d \to a + b$, $c + \bar{a} \to \bar{d} + b$, $c + \bar{b} \to a + \bar{d}$. This situation corresponds closely to the one occurring in even-coupling theories [10]. There is only one free-particle process, however, in which one might expect detectable difference among these modes [11], namely the μ-meson decay. In Part 4·2, *b*), it will be shown in detail that actually all modes give the same result for the μ-decay.

4. – Physical predictions of the theory.

4·1. – The results of the preceding analysis can be summarized by stating that, according to our assumptions, each hypothesis yields essentially only one possible interaction that fulfills all the requirements for a universal Fermi-type interaction:

a) *Hypothesis* (S'_S, S'_T):

$$H = g\mathcal{A}J(cd/ab) + \text{Herm. Conj.} \tag{18}$$

b) *Hypothesis* (S'_S, S_T):

$$H_1 = g_1\mathcal{A}J_1(cd/ab) + \text{Herm. Conj.} \tag{19}$$

Actual computation exhibits the rather striking circumstance that both (18) and (19) yield *exactly* the same answer for any process involving free particles.

The starting point for any calculation, at least in the case of free fermions, is the knowledge of the sum over all spins of $|H|^2$. This is an elementary

---

[10] J. Tiomno and J. A. Wheeler: *Rev. Mod. Phys.*, **21**, 144 (1949).

[11] The forbidden transitions in β-decay may provide additional discrimination among the three modes. At this stage, the lack of determination must be accepted as an unpleasant feature of the theory, which it is hoped to rectify later on.

but rather tedious business, because of the interference terms. We shall only make a few general remarks that may simplify future computations, and then state the final results. The Casimir projection operators are given by (we use natural units $\hbar = c = 1$ except for final numerical results):

$$D_{(a)} = \frac{1}{2}\left(1 + \boldsymbol{\alpha}\cdot\boldsymbol{v}_a \pm \beta\frac{m_a}{E_a}\right),$$

where $\boldsymbol{v}_a$ is the velocity of particle a; $\alpha^k = i\gamma^4\gamma^k$ and $\beta = \gamma^4$ satisfy the same relations (4) as γ^k and γ^4, which are characteristic of the Majorana representation. The following relations are of great practical help:

$$\bar{D}_{(a)} = D^*_{(a)} = \frac{1}{2}\left(1 + \boldsymbol{\alpha}\cdot\boldsymbol{v}_a \mp \beta\frac{m_a}{E_a}\right),$$

and, with

$$^{\pm}D^{\pm} = \frac{1}{2}\left(1 \pm \boldsymbol{\alpha}\cdot\boldsymbol{v} \pm \beta\frac{m}{E}\right):$$

$$\gamma^k\,{}^{\pm}D^{\pm} = {}^{\pm}D^{\mp}\gamma^k \mp i\gamma^4 v_k\,; \qquad \gamma^4\,{}^{\pm}D^{\pm} = {}^{\mp}D^{\pm}\gamma^4\,;$$

$$\gamma^5\,{}^{\pm}D^{\pm} = {}^{\pm}D^{\mp}\gamma^5\,; \qquad \alpha^k\,{}^{\pm}D^{\pm} = {}^{\mp}D^{\mp}\alpha^k \pm v_k\,.$$

The sum over all spins in case *a*) is given by

$$I = 2g^2\left[1 - \frac{m_a m_b m_c m_d}{E_a E_b E_c E_d} - (\boldsymbol{v}_a\cdot\boldsymbol{v}_b + \boldsymbol{v}_c\cdot\boldsymbol{v}_d) + (\boldsymbol{v}_a\cdot\boldsymbol{v}_b)(\boldsymbol{v}_c\cdot\boldsymbol{v}_d)\right]. \tag{20}$$

In (20), the energies E are all positive, and the term in which they appear carries the minus sign only if the process $c + d \to a + b$ involves even numbers of particles and antiparticles; odd numbers would require a plus sign. We shall, however, in the following take that term equal to zero, since one at least of the particles is a neutrino, which we assume to have mass zero. The same sum is given in case *b*) by:

$$I_1 = 2\cdot(4g_1)^2\left[1 - \frac{m_a m_b m_c m_d}{E_a E_b E_c E_d} - (\boldsymbol{v}_a\cdot\boldsymbol{v}_b + \boldsymbol{v}_c\cdot\boldsymbol{v}_d) + (\boldsymbol{v}_a\cdot\boldsymbol{v}_b)(\boldsymbol{v}_c\cdot\boldsymbol{v}_d)\right]. \tag{21}$$

Everything that has been said for (20) applies equally to (21). The two expressions are absolutely identical, save for the different normalization of the coupling constant, which exactly corresponds to what one would expect by comparing (16) and (17). The reason for this fact could be shown by a closer examination of the structure of (16) and (17).

The identity of (20) and (21) shows that both interactions yield the same numerical answers for free particles. The detailed comparison with all the experimental evidence available up to date is spared us by the very exhaustive work of McCallum and Wightman [9]. These authors examine which restrictions the known experimental data impose upon an a priori arbitrary linear combination of all five even or odd couplings. Their conclusion is that, both in the case of even and of odd couplings, there is only a unique linear combination not in conflict with experiment if two non-identical neutrinos occur in the μ-decay, namely $1/2(S + S' + T)$; if instead two identical neutrinos occur, there is a considerable arbitrariness, and both $\alpha T + \beta(S + S')$ or $\alpha T + \beta(V + 2S')$ are possible, with α and β *arbitrary* real numbers.

It is clear from (16) that (18) satisfies all the desired requirements. The situation, however, is too uncertain to consider their results as a definitive argument against (19). From (16) and (17) one sees that both interactions lead to Gamow-Teller selection rules; the great similarity of their structure has already been pointed out. One might think the hypothesis (S'_S, S_T) less symmetric than (S'_S, S'_T), and expect the final choice to be the interaction (18): this, of course, is no proof at all. We are investigating whether a decision on this point may still be reached on purely theoretical grounds.

We end this section by recording, for the sake of completeness, the sum over spins which results from the interaction $gJ + gJ' + g''J''$, without antisymmetrization, and which exhibits a remarkable symmetry:

$$
\begin{aligned}
I' = (g'')^2 \Big\{ 6 - 6\,\frac{m_a m_b m_c m_d}{E_a E_b E_c E_d} - 4(\boldsymbol{v}_a + \boldsymbol{v}_c)\cdot(\boldsymbol{v}_b + \boldsymbol{v}_d) + 2(\boldsymbol{v}_a\cdot\boldsymbol{v}_c + \boldsymbol{v}_b\cdot\boldsymbol{v}_d) + \\
+ 4[(\boldsymbol{v}_a\cdot\boldsymbol{v}_b)(\boldsymbol{v}_c\cdot\boldsymbol{v}_d) + (\boldsymbol{v}_a\cdot\boldsymbol{v}_d)(\boldsymbol{v}_b\cdot\boldsymbol{v}_c)] - 2[(\boldsymbol{v}_a\cdot\boldsymbol{v}_c)(\boldsymbol{v}_b\cdot\boldsymbol{v}_d)] \Big\} + \\
+ 4gg'' \Big\{ \boldsymbol{v}_b\cdot\boldsymbol{v}_c + \boldsymbol{v}_a\cdot\boldsymbol{v}_d - \boldsymbol{v}_a\cdot\boldsymbol{v}_b - \boldsymbol{v}_c\cdot\boldsymbol{v}_d - (\boldsymbol{v}_a\cdot\boldsymbol{v}_d)(\boldsymbol{v}_b\cdot\boldsymbol{v}_c) + \\
+ (\boldsymbol{v}_a\cdot\boldsymbol{v}_b)(\boldsymbol{v}_c\cdot\boldsymbol{v}_d) \Big\} + 2g^2 \Big\{ 1 - \frac{m_a m_b m_c m_d}{E_a E_b E_c E_d} - \\
- \boldsymbol{v}_a\cdot\boldsymbol{v}_c - \boldsymbol{v}_b\cdot\boldsymbol{v}_d + (\boldsymbol{v}_a\cdot\boldsymbol{v}_c)(\boldsymbol{v}_b\cdot\boldsymbol{v}_d) \Big\}.
\end{aligned}
$$

Again, the same remark applies to the mass term. Of course, taking both g and g'' equal to $1/2g$, I' reduces to (20), as it should because of (16).

Numerical results for processes (I).

4·2. – We report here the spectra for free neutron decay and μ-meson decay which follow from (20). As was already done in I, we omit consideration of the μ^--absorption, since the uncertainties of nuclear dynamics would not permit any conclusion of practical interest.

a) Neutron decay. – The spectrum for the decay of a free neutron at rest follows from

$$\underset{(N \text{ spin})}{Av\ I} = g^2 \left[1 - \frac{c\boldsymbol{p}_e}{E_e} \cdot \frac{c\boldsymbol{p}_P}{E_P} \right]$$

and is given to the first significant power of m_e/M, $[M = (M_N + M_P)/2]$, by

$$\mathrm{d}W = g^2 \frac{m_e^5 c^4}{2\pi^3 \hbar^7} \varepsilon \sqrt{\varepsilon^2 - 1} (\varepsilon_0 - \varepsilon)^2 \mathrm{d}\varepsilon \,, \tag{22}$$

with ε and ε_0 respectively the energy and maximum energy of the decay electron in units $m_e c^2$

In the case of complex nuclei the interactions (18) and (19) predict the correct spectra for forbidden transitions in the case of favorable parity change. This may not be the case for forbidden transitions with unfavorable parity change. There is clearly the need for further investigation of this subject; it might prove of decisive importance in selecting the correct interaction if further theoretical attempts to predict the unique interaction should fail.

b) μ-meson decay. – We consider the μ-meson at rest. It is of interest to remark the differences between the treatment of this process by means of pure even couplings ([10]) and the one that results from the interaction proposed here. In ref. ([10]), TIOMNO and WHEELER recognize three different possible modes of decay ([12]):

(ACE) « Antisymmetrical Charge Exchange »: $\begin{pmatrix} \mu^+ \\ \bar{e} \end{pmatrix} \to \begin{pmatrix} \nu' \\ \nu'' \end{pmatrix}$

(SCE) « Simple Charge Exchange »: $\begin{pmatrix} \mu^- \\ \bar{\nu}'' \end{pmatrix} \to \begin{pmatrix} \nu' \\ e \end{pmatrix}$

(CR) « Charge Retention »: $\begin{pmatrix} \mu^- \\ \bar{\nu}'' \end{pmatrix} \to \begin{pmatrix} e \\ \nu' \end{pmatrix}$.

([12]) Here, and only here, to adhere to their notations, the bar denotes a particle in a negative energy state, instead of the antiparticle regardless of the sign of its energy.

Each of the five couplings gives answers widely different for each of these modes. Only three combinations give results compatible with the experiment of SAGANE, *et al.* ([3]): ACE, tensor; CR, scalar and pseudoscalar.

In our theory we find, besides the fact that it is not necessary to specify the charge of the particles (this is a consequence of the charge-conjugation formalism: cfr. ref. ([2])), that: *a*) SCE and CR obviously coincide, *b*) the average over μ-meson spin of I turns out to be the same for all three modes:

$$\underset{(\mu\,\text{spin})}{\text{Av}}\ \text{I} = g^2[1 - \cos(\nu', \nu'')]\,.$$

All modes yields, therefore, the same spectrum:

$$\text{d}W = g^2\,\frac{m_e^4 m_\mu c^4}{4\pi^3\hbar^7}(\varepsilon_0 - \varepsilon)k^2\,\text{d}k\,, \tag{23}$$

(in (23) k is the electron momentum in $m_e c$ units, ε, ε_0 the energy and maximum electron energy in units $m_e c^2$ and $\varepsilon_0 = 1/2[m_\mu/m_e + m_e/m_\mu]$) and this is in good agreement with the experiment.

Cross sections for processes (II).

4·3. – These follow in a very simple form if we write

$$g = a^2\hbar c\,,$$

(a has the dimensions of a length). In the laboratory system, where the particle is at rest and the antiparticle has energy E, we find, for $m \neq 0$:

$$\sigma_{(\text{lab})_m} = 4\pi\left(\frac{a^2}{\lambda_c}\right)^2 \gamma\sqrt{\frac{\gamma+1}{\gamma-1}}\,, \tag{24}$$

with $\gamma = E/mc^2$, $\lambda_c = \hbar/mc$. For the reaction $\nu + \bar{\nu} \to \nu + \nu$ we find in the « c. m. system » (sum of initial momenta $= 0$):

$$\sigma_{(\text{cm})_\nu} = 8\pi\left(\frac{a^2}{\lambda_\nu}\right)^2\,, \tag{25}$$

λ_ν being the wavelength of one of the neutrinos in that system. The relative amount of neutrino-annihilations of pairs in matter with respect to photon-annihilations is of the order of about 10^{-7}.

4·4. – The idea of a universal interaction leads to the consideration of processes (II) as well as processes (I). The detection of the former is far beyond our present experimental possibilities; they might conceivably play a role together with the corresponding inverse processes, in cosmogonical problems.

The universal interaction, once its possibility has been recognized, appears in its most general form as a linear combination of all five odd couplings with real and imaginary constants. The requirement that it be antisymmetric in both the initial and final particles — which derives from the assumption that it should yield exactly the same formal treatment for all processes, whether involving identical particles or not — is the only one which eliminates in a consistent manner the imaginary constants and leads to only two mutually exclusive possibilities. It is hoped that a future investigation — based on arguments such as formulated in the Introduction, or on a further study of invariance properties — may lead to a final choice and thus set the whole question on a firmer ground.

We wish to point out, in conclusion, some of the questions which this investigation seems to us to open, to which we hope to return in the future. They only rest on the qualitative assumptions, stated already in I, which lead to processes (I) and (II).

1) It has been proved in Part 2 that the types under space and time inversions are intrinsic properties of the physical particles. From Tables I and II (Appendix), it appears that, in any case, electron and μ-meson must possess identical types: the processes

$$\mu + \bar{\mu} \to 2\nu$$
$$e + \bar{e} \to 2\nu$$
$$\mu + e \to 2\nu$$
$$e + \mu \to 2\nu$$
$$P + \mu \to N + \nu$$
$$P + e^- \to N + \nu$$

exhibit a striking symmetry. This seems to suggest a common nature of the two particles, e.g. that the μ-meson is an excited state of the electron.

2) No consideration has been given to the process of double β-decay, because the evidence for it is far from certain and we have been chiefly concerned with processes which would permit an immediate check on the theoretical predictions. Its study, however, appears quite feasible and of interest for a better understanding of the physical implications of the formalism.

Aknowledgment.

The author takes pleasure in extending his sincerest thanks to Dr. R. E. MARSHAK for his kind continued interest in this research and for many fruitful and interesting discussions, and to Mr. A. M. L. MESSIAH for very helpful criticism.

APPENDIX

TABLE I. – *Type assignments that exclude the unwanted processes in hypothesis* $(S'_S; S'_T)$.

$\mu = e$ / N		1	2	3	4
		$A_S A_T$	$A_S C_T$	$C_S A_T$	$C_S C_T$
1	$A_S A_T$	$B_S D_T$	$B_S B_T$	$C_S D_T$	$C_S B_T$
2	$C_S C_T$	$D_S A_T$	$D_S D_T$	$B_S A_T$	$B_S D_T$

The Table gives the type of P for ν type $= A_S C_T$ and N and $\mu = e$ as shown in the rows and columns.

The complete Table can be generated from I by adding to it the columns and rows that result by:

1) Applying to columns 1, 2, 3, 4 the substitution

$$\begin{pmatrix} A_S B_S C_S D_S \\ B_S A_S D_S C_S \end{pmatrix}.$$

2) Then applying to the resulting columns the substitution

$$\begin{pmatrix} A_T B_T C_T D_T \\ B_T A_T D_T C_T \end{pmatrix}.$$

3) and 4) Same operations with rows 1 and 2.

This yields 16×8 assignments, all corresponding to $\nu = A_S C_T$.

Once this is done, to each fixed assignment for e, μ, P there correspond still four possibilities for ν and N. These can be obtained by writing at the left of the column with the N types, the type $A_S C_T$ of ν, and then operating on the ν and N types as in 1) and 2). The four types thus obtained from

each ν, N assignment are completely equivalent to it in combinations with the other particles. Altogether, we find 672 possible assignments.

TABLE II. – *Same for hypothesis* (S'_S; S_T).

The complete Table follows by applying exactly the same procedure described above, starting from:

N \ $\mu = e$		1	2	3	4
		$A_S A_T$	$A_S C_T$	$C_S A_T$	$C_S C_T$
1	$A_S D_T$	$B_S D_T$	$B_S B_T$	$C_S D_T$	$C_S B_T$
2	$C_S A_T$	$D_S A_T$	$D_S D_T$	$B_S A_T$	$B_S D_T$

with the type of ν given now by $A_S A_T$.

RIASSUNTO

Si ricerca un'interazione universale tra tutti i noti fermioni, che escluda tutti i processi non occorrenti in natura a mezzo della sua invarianza rispetto a trasformazioni del gruppo di Lorentz ampliato. Si perviene, usando plausibili criteri di semplicità, a soltanto due interazioni, mutuamente esclusive, una almeno delle quali risulta in eccellente accordo con tutti i dati sperimentali noti fino ad oggi. Si dimostra inoltre che le due possibili interazioni danno identici risultati numerici nel caso di processi involventi particelle libere.

Sull'analisi statistica dei risultati di misure eseguite con contatori di Geiger.

L. Mezzetti

Centro di studio per la Fisica Nucleare del C.N.R., Istituto di Fisica dell'Università - Roma

R. Querzoli

Laboratorio di Fisica dell'Istituto Superiore di Sanità - Roma

(ricevuto il 19 Luglio 1951)

Riassunto. — Si espone un metodo per l'analisi statistica dei risultati di misure eseguite con gruppi di contatori di Geiger. Si deriva una formula che dà la probabilità che uno sciame di N particelle, incidendo su un gruppo di n contatori, ne scarichi ν (o almeno ν).

Per la interpretazione dei risultati di alcune misure, eseguite con contatori di G.M., sugli sciami di particelle generate dai raggi cosmici, ci si è recentemente presentato il problema di valutare la probabilità che uno sciame costituito da un numero N di particelle incidenti su un gruppo di n contatori, predisposti per rivelarle, ne colpisca un certo numero ν ($\leqslant n$). Poichè una tale formula non è deducibile a prima vista, e puó essere di qualche utilità nella interpretazione di esperienze consimili, la presentiamo nel seguito, insieme con la dimostrazione ed alcune valutazioni numeriche [1].

Sia p la probabilità che una particella ha di colpire un determinato contatore; assumeremo che tale probabilità sia la stessa per tutte le N particelle incidenti e per tutti gli n contatori. Ciò equivale ovviamente ad assumere che le N particelle incidano con distribuzione casuale entro un'area che comprende tutti i contatori, e che questi abbiano tutti la stessa area efficace.

L'espressione

$$s_n(N, \mu) = (1 - \mu p)^N$$

---

[1] Una formula più particolare, relativa al caso $\nu = n$ è stata data da Montgomery: *Journ. Frankl. Inst.*, **221**, 59 (1936).

rappresenta allora la probabilità complessiva di tutti gli eventi in cui un *determinato* gruppo di μ contatori non viene colpito da alcuna delle particelle incidenti. Indicheremo invece con $q_n(N, \mu)$ la probabilità di un evento in cui un determinato gruppo di μ contatori non viene colpito da alcuna particella, *mentre sono colpiti tutti i rimanenti* $\nu = n - \mu$.

Supponiamo ora che un determinato gruppo di k contatori non venga colpito e prendiamo in esame i rimanenti $h = n - k$. Supponiamo che di questi certi determinati α contatori non siano parimenti colpiti, mentre lo sono i rimanenti $h - \alpha$ ($\alpha = 0, 1, \ldots, h$). Scegliendo in tutti i modi possibili il gruppo di α contatori ed attribuendo ad α tutti i valori di cui è suscettibile, si ottengono evidentemente tutte le modalità, fra loro incompatibili, con cui si può verificare l'evento di probabilità $s_n(N, k)$. Per un dato valore di α la probabilità di una qualsiasi di queste modalità è evidentemente $q_n(N, k+\alpha)$, mentre il loro numero è $\binom{h}{\alpha} = \binom{n-k}{\alpha}$. Si ha pertanto:

$$(1) \qquad s_n(N, k) = \sum_0^{n-k} \binom{n-k}{\alpha} q_n(N, k+\alpha) = \sum_k^n \binom{n-k}{\beta-k} q_n(N, \beta) .$$

Moltiplichiamo ora ambo i membri della (1) per $(-1)^{\mu-k}\binom{n-\mu}{k-\mu}$ e sommiamo su tutti i valori di k fra μ ed n:

$$\sum_\mu^n {}_k (-1)^{\mu-k} \binom{n-\mu}{k-\mu} s_n(N, k) = \sum_\mu^n {}_k (-1)^{\mu-k} \binom{n-\mu}{k-\mu} \sum_k^n {}_\beta \binom{n-k}{\beta-k} q_n(N, \beta).$$

Invertendo a secondo membro l'ordine delle sommatorie, ed osservando che è:

$$\binom{n-\mu}{k-\mu}\binom{n-k}{\beta-k} = \binom{\beta-\mu}{k-\mu}\binom{n-\mu}{\beta-\mu},$$

si ottiene:

$$(2) \qquad \sum_\mu^n {}_k (-1)^{\mu-k} \binom{n-\mu}{k-\mu} s_n(N, k) = \sum_\mu^n {}_\beta \binom{n-\mu}{\beta-\mu} q_n(N, \beta) \sum_\mu^\beta {}_k (-1)^{\mu-k} \binom{\beta-\mu}{k-\mu} .$$

La seconda sommatoria a secondo membro non è altro che lo sviluppo di $(1-1)^{\beta-\mu}$ ed è quindi sempre uguale a zero tranne che per $\beta = \mu$, per cui vale 1; la (2) si riduce perciò alla:

$$(3) \qquad q_n(N, \mu) = \sum_\mu^n {}_k (-1)^{\mu-k} \binom{n-\mu}{k-\mu} s_n(N, k) .$$

La formula (3) permette di scrivere immediatamente la probabilità cercata. Indicando questa con $P_n(N, \nu)$ è infatti evidentemente:

$$P_n(N, \nu) = \binom{n}{\nu} q_n(N, \mu) \qquad (\mu = n - \nu)$$

che si può scrivere, in forma adatta per il calcolo numerico:

$$P_n(N, \nu) = \binom{n}{\nu} \sum_0^{\nu} {}_h (-1)^h \binom{\nu}{h} [1 - (n - \nu + h)p]^N . \tag{4}$$

Per $\nu = n$ la (4) si riduce alla formula data da MONTGOMERY e MONTGOMERY [1]. Si riconosce immediatamente che la $P_n(N, \nu)$ si annulla per $\nu > n$; si può inoltre dimostrare che essa si annulla anche, per ogni valore di n e di p, per $N < \nu$.

In certi casi può essere più comodo calcolare direttamente, anzichè la $P_n(N, \nu)$, la probabilità $\bar{P}_n(N, \nu)$ che «almeno ν» (cioè o ν o più di ν) degli n contatori siano colpiti. Essa si ottiene evidentemente facendo la somma

$$\bar{P}_n(N, \nu) = \sum_{\nu}^{n} {}_k P_n(N, k) . \tag{5}$$

La doppia sommatoria che compare nella (5) si può semplificare, sfruttando note relazioni fra i simboli combinatori, e si ottiene, in una forma comoda per il calcolo numerico

$$\bar{P}_n(N, \nu) = 1 - \sum_0^{\nu-1} {}_h (-1)^h \binom{\mu + h}{\mu} \binom{n}{\mu + h + 1} [1 - (\mu + h + 1)\, p]^N . \tag{6}$$

dove $\mu = n - \nu$.

Sia ora $f(N)$ la frequenza degli sciami incidenti contenenti N particelle. La frequenza degli eventi in cui ν degli n contatori, oppure «almeno ν» di essi sono colpiti (cioè, in una esperienza eseguita con contatori, le frequenze sperimentali) saranno rispettivamente:

$$\varphi(\nu) = \sum_{\nu}^{\infty} {}_N f(N) P_n(N, \nu) \qquad \nu = 1, 2, \ldots, n \tag{7a}$$

$$\bar{\varphi}(\nu) = \sum_{\nu}^{\infty} {}_N f(N) \bar{P}_n(N, \nu) . \tag{7b}$$

Se ci si propone di risalire dalle frequenze sperimentali alle frequenze $f(N)$, le (7) costituiscono un sistema di n equazioni con le infinite incognite $f(N)$; il problema è quindi insolubile se non si pongono altre condizioni, quali per esempio una limitazione per il numero massimo ammissibile di particelle costituenti uno sciame, o qualche ipotesi sulla forma della funzione $f(N)$, per lo meno per i valori $N > n$. In questo ultimo caso il problema è evidentemente suscettibile di trattazione numerica approssimata, con un metodo di approssimazioni successive.

Un caso particolare molto facile a trattare si ottiene se si assume che la distribuzione $f(N)$ sia poissoniana, intorno ad un numero medio M. Tenendo

conto del fatto che la $P_n(N, \nu)$ è identicamente nulla per ogni $N < \nu$ si può infatti scrivere:

$$\varphi(\nu) = \sum_0^\infty{}_N \exp[-M] \frac{M^N}{N!} P_n(N, \nu) .$$

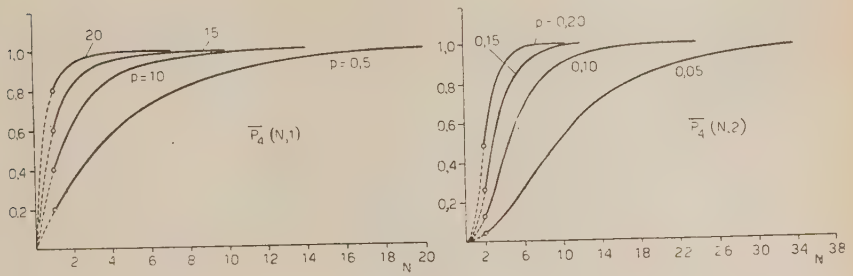

Fig. 1.

Invertendo la sommatoria rispetto ad N con quella che compare nella espressione di $P_n(N, \nu)$ si ottiene:

$$\varphi(\nu) = \exp[-M] \binom{n}{\nu} \sum_0^\nu (-1)^h \binom{\nu}{h} \sum_0^\infty{}_N \frac{M^N}{N!} [1 - (n - \nu + h)p]^N ,$$

da cui, con facili semplificazioni,

$$\varphi(\nu) = \binom{n}{\nu} \exp[-(n-\nu)Mp](1 - \exp[-Mp])^\nu . \tag{8}$$

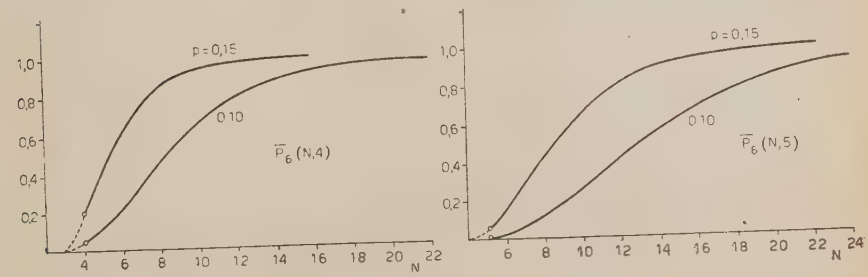

Fig. 2.

Si osservi che la (8) coincide, come deve, con la formula che esprime la probabilità che ν contatori, su n, siano colpiti quando sul gruppo incide uno sciame esteso di densitá media $\Delta = Mp/S$.

A titolo di esempio riportiamo il diagramma della $\overline{P}_\nu(N, \nu)$ per alcuni valori di n, ν e del parametro p.

Appendice

1. – $P_n(N, \nu) \equiv 0$ *per* $N < \nu$.

Sviluppando la potenza $[1 - (n - \nu + h)p]^N$ la (4) diventa, dopo inversione dell'ordine delle sommatorie

$$P_n(N, \nu) = \binom{n}{\nu} \sum_0^N{}_j (-1)^j \binom{N}{j} p^j \sum_0^\nu{}_h (-1)^h \binom{\nu}{h} (n - \nu + h)^j . \tag{9}$$

Se $N < \nu$, anche $j < \nu$. Ora si può dimostrare facilmente che è:

$$\sum_0^\nu{}_h (-1)^h \binom{\nu}{h} (\mu + h)^j \equiv 0 \qquad \text{per } j = 0, 1, 2, \ldots, \nu, \tag{10}$$

con il che l'asserto è dimostrato. Per dimostrare la (10) basta osservare che si può scrivere:

$$(\mu + h)^j = [D^{(j)} \exp [(\mu + h)]x]_{x=0},$$

dove $D^{(j)}$ indica derivazione d'ordine j rispetto ad x. La (10) diventa allora:

$$\left[D^{(j)} \sum_0^\nu{}_h (-1)^h \binom{\nu}{h} \exp [(\mu + h)x]\right]_{x=0} = [D^{(j)} \exp [\mu x](1 - \exp [x])^\nu]_{x=0} .$$

Ora tutte le derivate, fino all'ordine $\nu - 1$, dell'espressione $\exp [\mu x](1 - \exp [x])^\nu$ contengono un fattore $(1 - \exp [x])^\alpha$, con $\alpha = \nu, \nu - 1, \ldots 1$, che si annulla per $x = 0$; il che prova l'asserto.

2. – *Dimostrazione della* (6).

Per la (4) e la (5) è:

$$\bar{P}_n(N, \nu) = \sum_0^{n-\nu}{}_k \binom{n}{k} \sum_0^k{}_j (-1)^{n-k-j} \binom{k}{j} [1 - (n - j)p]^N,$$

Invertendo l'ordine delle sommatorie si ottiene

$$\bar{P}_n(N, \nu) = \sum_0^{\nu-1}{}_j (-1)^{n-j} [1 - (n - j)p]^N \binom{n}{j} \sum_0^{n-\nu}{}_k (-1)^k \binom{n-j}{k} +$$
$$+ \sum_\nu^n{}_j (-1)^{n-j} [1 - (n - j)p]^N \binom{n}{j} \sum_0^{n-j}{}_k (-1)^k \binom{n-j}{k} .$$

Si verifica immediatamente che il secondo termine vale 1 perchè la sommatoria rispetto a k si annulla identicamente per ogni j tranne che per $j = n$,

per cui vale 1. Per valutare il primo termine basta osservare che

$$\sum_0^{n-\nu}{}_k (-1)^k \binom{n-j}{k} = 1 + \sum_1^{n-\nu}{}_k (-1)^k \left[\binom{n-j-1}{k-1} + \binom{n-j-1}{k}\right]$$

e che ogni termine della sommatoria a secondo membro si elide per metà con il precedente e per metà col successivo, tranne il primo e l'ultimo che danno

$$\sum_0^{n-\nu}{}_k (-1)^k \binom{n-j}{k} = 1 + \left[-1 + (-1)^{n-\nu}\binom{n-j-1}{n-\nu}\right] = (-1)^{n-\nu}\binom{n-j-1}{n-\nu}.$$

Si ottiene perciò:

$$(11) \qquad \overline{P}_n(N,\nu) = 1 + \sum_0^{\nu-1}{}_j (-1)^{2n-\nu-j}\binom{n}{j}\binom{n-j-1}{n-\nu}[1-(n-j)p]^N .$$

La (11), come si riconosce immediatamente, coincide con la (6).

SUMMARY

A method for the statistical treatment of the results of G.M.-counter measurements is given. A formula giving the probability that a shower of N particles discharges ν out of n counters is derived.

High energy nuclear interactions of cosmic ray particles close to the top of the atmosphere. (*)

M. L. Vidale and M. Schein

Department of Physics, University of Chicago (U.S.A.)

(ricevuto il 24 Luglio 1951)

Summary. - A study of the altitude and latitude dependence of the various cosmic ray components provides information on the nature of high energy nuclear interactions of cosmic ray particles close to the top of the atmosphere. Counter telescopes have been flown with plastic balloons to a maximum altitude of 94 000 ft. Intensity vs. pressure curves have been obtained at geomagnetic latitudes of $\lambda = 55°$, 41° and 28° for the total cosmic radiation and for the components capable of traversing 4, 7.5 and 12 cm of lead. The energy spectrum of primary cosmic ray particles has been derived from the extrapolation of the intensity of the total radiation to the top of the atmosphere. The integral momentum spectrum of the total primary radiation is given by $N(>pc/Ze) = 0.48(pc/Ze)^{-1.0}$. Subtracting the known contribution of primary α-particles and heavier nuclei the spectrum of primary protons becomes $P(>pc/e) = 0.43(pc/e)^{-1.0}$. Results indicate that the radiation originating from primaries in the energy range of 1 to 4 GeV (cutoff energies at $\lambda = 55°$ and 41°) is predominantly of a nucleonic nature. The absence of an electronic component can be explained by assuming that, close to the top of the atmosphere, electrons originate predominantly from the decay of neutral mesons and that in this energy range the probability of producing mesons is quite small. In sharp contrast, the soft component originating from primaries in the range of 4 to 8 GeV (cutoff at $\lambda = 41°$ and 28°) multiplies rapidly in the atmosphere. This large transition effect in air with a maximum at about 10 cm Hg pressure is characteristic of electron showers. It is concluded that the probability of producing neutral mesons singly reaches nearly its saturation value at energies of the primary radiation between 4 and 8 GeV. At energies higher than 8 GeV this effect is even more pronounced due to the contribution of the plural production of mesons. In order to study the production of mesons in the interaction of cosmic ray particles with a liquid Hydrogen target, a counter experiment

(*) Assisted by the joint program of the Office of Naval Research and the Atomic Energy Commission.

was carried out at an altitude of 90,000 ft. During the first half of the experiment, an average of 1.6 g/cm² of Hydrogen was interposed between the counters. The Hydrogen was then ejected and data obtained during the remaining portion of the flight at altitude. From the narrow angular distribution of the events originating in liquid Hydrogen (total angular spread $\sim 15°$), sharply different from those originating in the walls of the Dewar container (minimum angular spread $\sim 50°$), it is concluded that they were produced by very high energy primary particles. It is estimated that the events in Hydrogen resulted mostly (80%) from the interaction of primary protons of an average energy of 50-100 GeV in which a minimum of four mesons were produced. Penetrating showers in lead have been investigated at $\lambda = 55°$ and 28°. Between these two latitudes, at an atmospheric pressure of 1.5 cm Hg, the ratio of the radiation producing penetrating showers amounts to 1.5, as compared to 2.9 for the hard component and 4.1 for the total radiation.

1. – Introduction.

Several experiments have been performed in an attempt to gain a better understanding of nuclear events leading to the production of mesons and secondary nucleons. Energies sufficient to create several mesons in a single nuclear interaction are available at present only in the cosmic radiation (1). Since different types of particles are in general absorbed in matter with a different mean free path, it can be expected that a study of the intensity of the cosmic radiation as a function of altitude, latitude and penetrability in lead will provide information regarding the nature of the various cosmic ray components. In order to obtain more direct information on meson production in proton-proton collisions, multiple events originating in a liquid Hydrogen target were investigated.

MILLIKAN and his collaborators (2) have made extensive measurements of the total intensity of the cosmic radiation in a series of balloon flights at various latitudes. The hard component has been studied by SCHEIN and collaborators (3) in a number of investigations using counter telescopes with lead absorbers of several thicknesses interposed between the counters. Experiments of a similar nature have been performed by other workers during the

(1) J. J. LORD, J. FAINBERG and M. SCHEIN: *Phys. Rev.*, **80**, 970 (1950).
(2) R. A. MILLIKAN, H. V. NEHER and W. H. PICKERING: *Phys. Rev.*, **61**, 396 (1942).
(3) M. SCHEIN, W. P. JESSE and E. O. WÖLLAN: *Phys. Rev.*, **59**, 615 (1941).

past few years ([4,5,6,7,8]). In view of many recent improvements in balloon techniques which permit the study of the cosmic radiation up to a pressure of less than 15 g/cm², it was considered advisable to conduct a further series of flights using counter telescopes of similar geometry so as to obtain results which were strictly comparable. In these flights the total, soft, and hard component were measured simultaneously using a technique previously reported by M. SCHEIN at the Pasadena conference ([9]). This technique permits the comparison of the various components of the cosmic radiation under identical atmospheric conditions. Furthermore time variations in the intensity of the cosmic radiation due to solar activity and other sources can be recognized by the fact that the variations are not the same for the various components.

The simultaneous emission of several mesons and nucleons in high energy nuclear collisons has been studied both at lower altitudes ([10,11]) and at balloon elevations ([12,13,14]) using counter arrangements and photographic emulsions. By the study of small angle scattering along the tracks in nuclear emulsions it was found ([14]) that most (80 to 90%) of the relativistic particles ejected in such nuclear encounters consist of π-mesons with some contribution of protons. A number of theories have been proposed to describe phenomena of this kind. Some of these theories predict multiple meson production from a single nucleon-nucleon collision ([15,16,17]) (multiple production), others assume that only one meson originates in a single nuclear collision and interpret meson showers as resulting from nucleonic and mesonic cascades within a

---

([4]) M. POMERANTZ: *Phys. Rev.*, **69**, 75 (1949).

([5]) J. R. WINCKLER, T. STIX, K. DWIGHT and R. SABIN: *Phys. Rev.*, **79**, 656 (1950).

([6]) K. S. CHANDRASEKHAREN, G. S. GOKHALE and A. S. RAO: *Proc. Indian Acad. Sci.*, **32A**, 95 (1950).

([7]) G. S. GOKHALE, A. W. PEREIRA and A. S. RAO: *Proc. Indian Acad. Sci.*, **32A**, 98 (1950).

([8]) M. VIDALE and M. SCHEIN: *Phys. Rev.*, **81**, 1065 (1951).

([9]) J. R. OPPENHEIMER: *Rev. Mod. Phys.*, **21**, 181 (1949). Results to be published soon.

([10]) G. WATAGHIN, M. DE SOUZA SANTOS and P. A. POMPEIA: *Phys. Rev.*, **57**, 61 (1940).

([11]) L. JANOSSY, and P. INGLEBY: *Nature*, **145**, 511 (1940).

([12]) M. SCHEIN, M. IONA and J. TABIN: *Phys. Rev.*, **64**, 253 (1943).

([13]) J. J. LORD and M. SCHEIN: *Phys. Rev.*, **77**, 19 (1950).

([14]) U. CAMERINI, P. H. FOWLER, N. O. LOCK and H. MUIRHEAD: *Phil. Mag.*, **41**, 413 (1950).

([15]) H. W. LEWIS, J. R. OPPENHEIMER and S. A. WOUTHUYSEN: *Phys. Rev.*, **73**, 127 (1948).

([16]) W. HEISENBERG: *Nature*, **164**, 65 (1949).

([17]) E. FERMI: *Prog. Theor. Phys.*, **5**, 570 (1950).

single nucleus ([18]) (plural production). In particular, the statistical theory of FERMI ([17,19]) gives a quantitative account of the multiplicity of meson production and the angular distribution of the emitted particles which is in good agreement with recent experimental evidence in photographic emulsions ([1,14]). These and other recent investigations ([20]) strongly favor multiple meson production in a single nucleon-nucleon collision. However, since emulsions contain elements of different atomic weights, a counter experiment was performed to study the production of mesons in the interaction of primary cosmic rays with a liquid Hydrogen target. Experiments of this kind are somewhat complicated by the fact that the primary radiation consists of approximately 80÷90% protons ([3]), 19÷9% α-particles and 1% heavier nuclei ([21,22]). Since electrons have been shown to be present only in negligible amounts close to the top of the atmosphere ([3,23,24]) and the intensity of high energy nuclei decreases rapidly with increasing atmospheric pressure, the counter experiment designed to detect multiple events originating in liquid Hydrogen was carried out at an altitude of 90 000 ft. At lower elevations the presence of electronic showers causes considerable difficulties in observing the effect in Hydrogen. In order to compare showers originating in liquid Hydrogen with those in nuclei of higher atomic number in which successive collisions can occur inside the same nucleus, the production of penetrating showers in lead was investigated at $\lambda = 55°$ and $28°$.

2. – Balloon flight techniques.

The apparatus, consisting of the counters, coincidence circuits, power packs and recording unit was mounted inside a light Dow-metal frame covered with pyraline, a transparent plastic very opaque to infrared radiation. Bands of Aluminum foil around the gondola reflected the proper amount of solar radiation to maintain the equipment close to room temperature. During the flight a record was kept of the temperature inside the gondola, which showed that in most cases the temperature averaged about 20 °C.

Each apparatus was tested inside a large tank which was evacuated down to a pressure of 0.5 cm Hg, a pressure lower than the lowest pressure reached in the balloon flights. This was done in order to check the performance of

([18]) W. HEITLER and L. JANOSSY: *Helv. Phys. Acta*, **23**, 417 (1950).
([19]) E. FERMI: *Phys. Rev.*, **81**, 683 (1951).
([20]) E. PICKUP and L. VOYVODIC: *Phys. Rev.*, **82**, 265 (1951).
([21]) P. FREIER, E. J. LOFGREN, E. P. NEY, F. OPPENHEIMER, H. L. BRADT and B. PETERS: *Phys. Rev.*, **74**, 213 (1948).
([22]) B. PETERS: Private communication to M. SCHEIN.
([23]) R. HULSIZER and B. ROSSI: *Phys. Rev.*, **73**, 1402 (1948).
([24]) C. L. CRITCHFIELD, E. P. MEY and S. OLOSKA: *Phys. Rev.*, **79**, 402 (1950).

the circuits under conditions similar to those found in the stratosphere; in particular, to guarantee that corona discharges could not occur across the high voltages required for the operation of the Geiger counters.

The counter equipment used in these investigations was flown with plastic, constant level balloons manufactured by the General Mills Company. The balloons were followed in flight by an airplane. The cosmic ray equipment was released from the balloon at a predetermined time and dropped to the ground by parachute. The apparatus was promptly recovered in every case. The essential characteristics of each flight are summarized in Table I.

TABLE I.

Flight Number	Type of Experiment	Date	Geom. Lat.	Duration of Flight (Hours)	Rate of Ascent (ft/min)	Max. Altitu	
						cm Hg pressure	ft
I	counter telescope CT_1	Nov. 15, 1949	28°	$8\,^3/_4$	670	1.1	94
II	counter telescope CT_1	June 6, 1950	55°	$10\,^1/_2$	330 to 60 000 ft 160 above 60 000 ft	1.6	86
III	counter telescope CT_2	Aug. 4, 1950	55°	$8\,^1/_2$	710	1.2	93
IV	Multiple Events in Hydrogen	Sept. 6, 1950	52°	$6\,^1/_2$	1 000	1.4	91
V	counter telescope CT_3	Jan. 13, 1951	41°	6	120	4.0	66
VI	counter telescope CT_3	Feb. 4, 1951	41°	$6\,^1/_2$	450	1.7	84

In every flight pressure readings were obtained by two or more independent methods. In all cases the pressure data obtained with the various instruments were within experimental error. The pressure measuring devices consisted of:

1) Barograph with temperature compensated elements.

2) Radiosonde or Olland cycle type barometer which transmitted pressure data to the ground station.

3) On flights IV, V and VI (see Table I) two mercury U-tubes were photographed at 10 minute intervals. The U-tubes gave very accurate ($\sim$ .3 mm Hg) altitude data for pressure lower than 12 cm Hg (*).

3. – Intensity of the cosmic ray components.

3·1. – *Description of the Apparatus.* – The counter telescopes used for the measurement of the vertical intensity of the cosmic radiation are shown in Fig. 1. Each apparatus contained several vertical telescopes of Geiger-Müller

(*) On some occasions the altitude of the balloon could be estimated by means of theodolite readings or radar tracking.

counters arranged to detect fourfold coincidences. Equipment CT_1 and CT_2 (see Fig. 1) recorded coincidences of the type *ABCD*, *BCDE*, *BCDF* and *BCDG*, while equipment CT_3 recorded coincidences *ABCD*, *BCDE*, *CDEF* and *DEFG*.

All Geiger-Müller counters were 2.4 cm in diameter and had an active length of 12.5 cm. The distance between the centers of the two extreme counters in each of the fourfold vertical telescopes was the same and amounted to 28 cm. Assuming that all particles are incident on the equipment isotropically, the correction to be applied to the measured vertical cosmic ray intensity due to the finite dimensions of the counter telescopes can be shown to amount to less than 2%. The effect on solid angle calculations of particles giving rise to secondaries in the lead blocks interposed between the counters will be discussed in a later section.

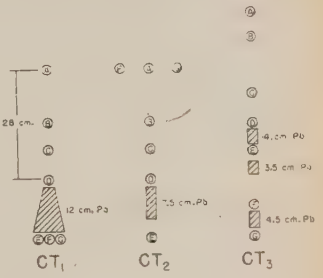

Fig. 1. – Counter telescopes used for the measurement of the intensity of the cosmic ray components and of the penetrating showers originating in lead.

The wall thickness of the brass counters used was 0.08 cm. Hence, in order to produce a fourfold coincidence, an incident particle, depending on its direction, had to penetrate a minimum of 5 to 7 g/cm² of brass.

Each fourfold coincidence caused the flash of a neon bulb which was separately recorded as a narrow line on a photographic film. The film was mounted on a rotating drum driven by a clock mechanism. Two coincidences could be resolved if they occurred more than 0.25 s apart. Corrections arising from the finite resolving time of the recorder are quite negligible except in the measurement of the intensity of the total component at high latitude; however, they were taken into account for all cases. Often more than one neon bulb flash appeared on the film, indicating the simultaneous occurrence of several fourfold coincidences. Such multiple coincidences could be resolved within 0.5 s.

The length of the coincidence pulses of the circuits used in the equipment was 30 μs. Due to the fact that only fourfold coincidences were recorded the number of accidentals was reduced to a negligible fraction of the counting rate of the telescopes.

The temporary inactivation of the counters following each discharge was determined in the laboratory under conditions similar to those found in the stratosphere by placing a radium source a certain distance from the counters. This dead time reduces the fourfold counting rate by approximately 5% at a single counter counting rate of 60 counts/s. Losses due to dead time for

a single counter were estimated from the intensity of the cosmic radiation as a function of altitude.

The individual counter telescopes were accurately tested in the laboratory at Chicago before each balloon flight. Since the telescopes which were designed to have the same geometry gave the same counting rate within a statistical error of 3%, it was concluded that the individual counters were lined up correctly. Tests were also made to guarantee that the lead blocks covered the active area of the counters completely. As an example, the counting rate of the counter telescope CT_3 (Fig. 1) is given in Table II for various thicknesses of lead absorber as obtained in Minneapolis (Geomagnetic latitude $\lambda = 55°$, 600 ft elevation above sea level) and in White Sands, New Mexico ($\lambda = 41°$, 4100 ft elevation).

TABLE II. – *Ground Counting Rate of Standard Telescopes.*

Thickness of absorber (cm of Pb)	Counts/min	
	Minneapolis	White Sands
0	.700 ± .02	.880 ± .03
4	.605 ± .02	.787 ± .03
7.5	.567 ± .02	.663 ± .03
12	.525 ± .02	.616 ± .03

3·2. – *Experimental results.* – In a series of balloon flights (see Table I) at 55°, 41° and 28° N Geomagnetic latitude, the intensity of the various cosmic ray components was measured as a function of altitude using counter telescopes with varying amounts of lead interposed between the counters. In most of the flights the rate of rise of the balloon was sufficiently low to

TABLE III. – 55° *Geomagnetic Latitude.*

Pressure (cm Hg)	0 cm Pb absorber (counts/min)	Pressure (cm Hg)	7.5 cm Pb absorber (counts/min)	Pressure (cm Hg)	12 cm Pb absorber (counts/min)
1.3	20.7 ± .2	1.2	12.0 ± .2	1.6	10.3 ± .3
2.2	22.5 ± .7	2.7	12.8 ± .7	2.2	10.1 ± .3
3.2	23.5 ± .6	7.4	10.7 ± .6	4.8	10.7 ± .7
5.6	26.1 ± .7	17.0	4.8 ± .6	5.8	9.9 ± .8
10.9	20.1 ± .5	28.0	2.4 ± .8	7.5	9.1 ± 1.0
24.7	7.8 ± .5	—	—	9.3	8.4 ± .7
31.0	4.4 ± .5	—	—	11.9	6.9 ± .7
—	—	—	—	15.0	5.2 ± .7
—	—	—	—	19.5	2.7 ± .5
—	—	—	—	25.0	2.5 ± .4
—	—	—	—	31.0	1.9 ± .4

give statistically significant data for the dependence of cosmic ray intensity on altitude. As a consequence, this series of flights had considerable advantages over those of previous investigators in studying cosmic ray components of low intensity and in considering differences between counting rates of various components at one particular altitude.

Tables III and IV give the counting rate of the fourfold coincidences in

TABLE IV.

41° Geom. Lat.					28° Geom. Lat.			
Pressure (cm Hg)	0 cm Pb absorber (cnts/min)	4 cm Pb absorber (cnts/min)	7.5 cm Pb absorber (cnts/min)	12 cm Pb absorber (cnts/min)	Pressure (cm Hg)	0 cm Pb absorber (cnts/min)	12 cm Pb absorber (cnts/min)	
1.9	9.2 ± .3	7.5 ± .2	5.6 ± .2	4.8 ± .2	1.2	5.0 ± .1	3.6 ± .1	
5.0	13.4 ± .5	9.1 ± .4	6.8 ± .3	5.4 ± .3	2.2	5.7 ± .4	3.6 ± .3	
8.6	15.4 ± .5	8.3 ± .3	6.3 ± .3	5.4 ± .3	6.1	8.8 ± .5	4.3 ± .3	
13.9	13.6 ± .6	7.2 ± .4	5.1 ± .4	3.7 ± .3	12.6	9.4 ± .9	4.1 ± .6	
20.6	11.1 ± .4	5.3 ± .3	3.6 ± .2	3.3 ± .2	17.3	6.0 ± .5	3.8 ± .5	
23.0	8.2 ± .6	4.6 ± .5	3.5 ± .5	2.5 ± .4	25.0	5.6 ± .6	2.1 ± .4	
38.0	3.2 ± .2	2.3 ± .2	1.8 ± .2	1.8 ± .2	35.0	2.3 ± .5	1.5 ± .3	

telescopes CT_1, CT_2 and CT_3 (see Fig. 1) at $\lambda = 55°$, 41° and 28°. Each value has been corrected for accidental coincidences, dead time losses and losses due to the resolving time of the recording unit as discussed in section 3·1. The error given for each experimental point represents the standard error obtained from the square root of the number of counts registered in the individual telescopes.

Curves T_{55}, T_{41} and T_{28} in Figs. 2, 3 and 4 are plots of the total vertical intensity of the cosmic radiation at the three latitudes of $\lambda = 55°$, 41° and 28° respectively. For comparison these curves are presented together in Fig. 5. All three curves show a pronounced maximum which occurs at an increasing altitude at higher latitudes.

Curves H_{55}, H_{41} and H_{28} in Figs. 2, 3 and 4 represent the vertical intensity of the penetrating component of the cosmic radiation capable of traversing 12 cm of lead. These three curves are given in Fig. 6 where it appears that the intensity of the penetrating component increases

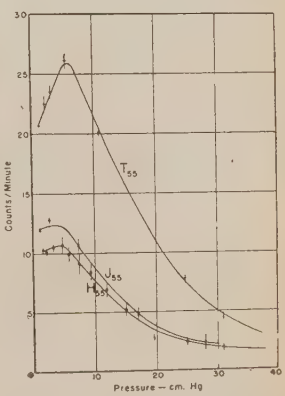

Fig. 2. – Altitude dependence of the intensity of the cosmic radiation at $\lambda = 55°$ as measured through 0 cm of lead (T_{55}), 7.5 cm of lead (J_{55}) and 12 cm of lead (H_{55}).

down to a pressure of 5, 9 and 15 cm Hg at $\lambda = 55°$, 41° and 28° respectively. At lower pressures all three curves show a very flat maximum which extends to the highest altitudes reached in the flights.

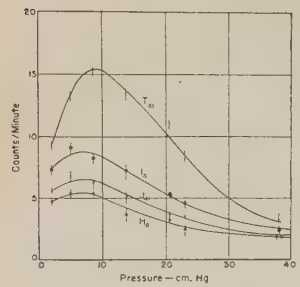

Fig. 3. – Altitude dependence of the intensity of the cosmic radiation at $\lambda = 41°$ as measured through 0 cm of lead (T_{41}), 4 cm of lead (I_{41}), 7.5 cm of lead $J_{(41)}$ and 12 cm of lead (H_{41}).

The vertical intensity through 4 and 7.5 cm of lead was measured in order to obtain intermediate points between the total and the hard component. The intensity of the cosmic radiation through 4 cm of lead was obtained at $\lambda = 41°$ (curve I_{41} in Fig. 3) and through 7.5 cm of lead at $\lambda = 55°$ and 41° (curves J_{55} and J_{41} in Figs. 2 and 3). Curves I_{41} and J_{41} exhibit a maximum at about 7 cm Hg pressure and in general show very similar characteristics. Curve J_{55} is very similar to the hard component curve at $\lambda = 55°$. It is of interest to find maxima in the vertical intensity as measured through 7.5 and 12 cm of lead, a result which other investigators have not obtained. This may be due to the fact that the flights reported here had a very low rate of rise and spent a considerable time at pressures of less than 6 cm Hg.

The magnetic field of the earth determines, as a function of latitude, the minimum energy that charged cosmic ray particles must have to enter the atmosphere from outer space ([25,26]). This cutoff energy for particles incident from the vertical direction at $\lambda = 55°$, 41° and 28° is given in Table V.

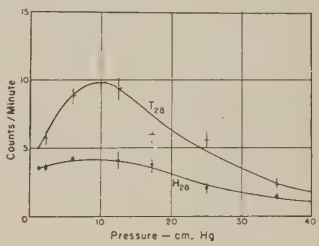

Fig. 4. – Altitude dependence of the intensity of the cosmic radiation at $\lambda = 28°$ as measured through 0 cm of lead (T_{28}) and 12 cm of lead H_{28}).

TABLE V. – *Geomagnetic cutoff of primary cosmic rays from the vertical direction.*

Geomagnetic latitude	Proton Energy (GeV)	Heavy nuclei ($Z \geqslant 2$) Energy per nucleon (GeV)
55°	1.0	0.35
41°	4.0	1.5
28°	8.2	3.5

([25]) M. S. VALLARTA *Phys. Rev.*, **74**, 1837 (1948).
([26]) R. A. ALPHER: *Journ. of Geophys. Rev.*, **55**, 437 (1950).

From the known geometry of the counter telescopes, the vertical flux (number of incident particles/cm² sterad s) of the cosmic radiation was calculated using the following formula:

$$B = \frac{a^2 b^2}{l^2}\left[1 - \frac{a^2 + b^2}{3l^2}\right],$$

where B is the area times solid angle product for the counter telescope used, a and b are the counter dimensions and l the overall separation of the counters

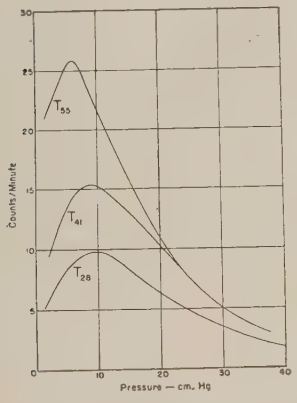

Fig. 5. - Altitude dependence of the total cosmic radiation at $\lambda = 55°$ (T_{55}), $\lambda = 41°$ (T_{41}) and $\lambda = 28°$ (T_{28}).

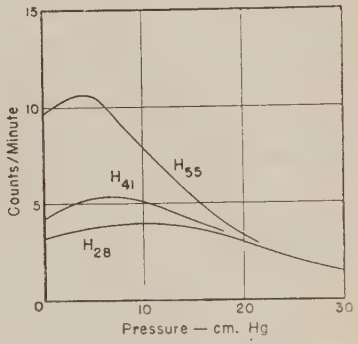

Fig. 6. - Altitude dependence of the hard component of the cosmic radiation as measured through 12 cm of lead at $\lambda = 55°$ (H_{55}). $\lambda = 41°$ (H_{41}) and $\lambda = 28°$ (H_{28}).

Table VI gives the flux of the primary radiation vertically incident on the atmosphere at $\lambda = 55°$, 41° and 28° as extrapolated from the known shape of the intensity curve of the total radiation to the top of the atmosphere.

TABLE VI. - *Primary flux of the cosmic radiation.*

Flux/cm² sterad · s	$\lambda = 55°$	$\lambda = 41°$	$\lambda = 28°$
Total primary flux	0.296 ±.02	0.102 ± .02	0.059 ± .02
Proton flux	0.27 ±.02	0.09 ± .02	0.05 ± .02

The total primary flux is well represented by a power law of the following type:

$$N\left(> \frac{pc}{Ze}\right) = 0.48 \left(\frac{pc}{Ze}\right)^{-1.0 \pm .1},$$

where N is the integral spectrum of particles of magnetic rigidity greater than pc/Ze. This spectrum is in very good agreement with recent measurements of the total cosmic radiation made above the atmosphere in experiments with rockets ([27]) using counter telescopes of rather wide geometry. This agreement indicates that the extrapolation made in order to obtain the flux of the primary cosmic radiation at the top of the atmosphere is justified. It also indicates that in experiments with rockets, the rocket does not contribute appreciably to the intensity of the cosmic radiation as measured with counter telescopes. This primary spectrum can also be compared to the results obtained by WINCKLER ([28]) using telescopes with 3 cm of lead interposed between the counter trays. However, due to the absorption in lead of a fraction of the radiation of lower energy, the flux given by WINCKLER at 55° is 25% lower than the flux found with counter telescopes without lead absorber.

Subtracting from the intensity of the total primary cosmic radiation the contribution of primary α-particles and heavy nuclei recently measured with nuclear emulsions by B. PETERS ([22]), one obtains the flux of primary protons given in Table VI. This flux can be represented by a power law of the following type:

$$P\left(>\frac{pc}{e}\right)=0.43\left(\frac{pc}{e}\right)^{-1.0\pm.1},$$

where P is the integral spectrum of primary protons of magnetic rigidity greater than pc/e.

The latitude effect $\left(\frac{\text{Intensity at } \lambda = 55^\circ \text{ or } 41^\circ}{\text{Intensity at } \lambda = 28^\circ}\right)$ of the intensity of the total and hard component of the cosmic radiation at $\lambda = 55^\circ$ and 41° is given in Table VII for a few selected altitudes in the atmosphere. It appears that at all altitudes the total radiation shows a larger latitude effect than the hard

TABLE VII. – *Latitude effect of the total and hard components.*

Pressure (cm Hg)	55° Geom. Lat.		41° Geom. Lat.	
	Total	Hard	Total	Hard
0	4.9	3.0	1.7	1.3
1.2	4.2	2.8	1.7	1.3
6	2.9	2.5	1.6	1.3
10	2.2	1.8	1.5	1.2

([27]) J. A. VAN ALLEN and S. F. SINGER: *Phys. Rev.*, **78**, 819 (1950).
([28]) J. R. WINCKLER, T. STIX, K. DWIGHT and R. SABIN: *Phys. Rev.*, **79**, 656 (1950).

component. Also, for both components, the latitude effect reaches a maximum at the top of the atmosphere. As the primary radiation has, in all probability, a larger latitude effect than any of the other cosmic ray components, one can conclude that the total radiation will give the most reliable information on the relative intensity of the primary flux at various latitudes.

The intensity vs. altitude curves obtained at $\lambda = 55°$ (Fig. 2) do not extrapolate to a common point at the top of the atmosphere. At $\lambda = 41°$ and 28° (see Figs. 3 and 4) the effect is somewhat similar, but less pronounced because of the considerably higher cutoff energy of the primary radiation. At $\lambda = 55°$ the difference in the extrapolated intensity of the total and hard components amounts to approximately 50%, as compared to 35% at $\lambda = 41°$ and 15% at $\lambda = 28°$. This effect can be explained by noting that primary cosmic ray particles incident on the equipment at these latitudes interact with nuclei of the lead absorber. These interactions, which are known to occur with a collision cross-section equal to the geometrical area of the lead nuclei, lead to the emission of secondary particles which in turn can be absorbed or scattered out of the counter telescope. At low latitudes, where the primary particles have a higher average energy, this effect is considerably smaller as secondary particles produced in the 12 cm of lead have often sufficient energy to traverse the remaining amount of lead and trigger the lower counters of the telescope. It appears therefore, that even a small amount of absorber in the counter telescope may stop low energy primaries and that the extrapolated flux obtained with such telescopes may be considerably lower than the total primary flux.

It should be noted that at high altitude the penetrating component of the cosmic radiation consists predominantly of two types of particles, protons and μ-mesons. If the absorber used in the experiment to select penetrating particles has a thickness of the order of a collision mean free path, the probability is high that protons will interact in the absorber and produce secondaries which may trigger counters not in line with the incident particles. As a consequence, close to the top of the atmosphere where high energy protons make up a large fraction of the penetrating radiation, the intensity of the hard component may have been seriously overestimated.

From Figs. 2, 3 and 4, one can obtain the difference curves representing the contribution to the intensity of the cosmic radiation of primaries in the energy ranges 1 to 4 GeV (cutoff energies at $\lambda = 55°$ and 41°), 4 to 8 GeV (cutoff at $\lambda = 41°$ and 28°) and > 8 GeV (cutoff at $\lambda = 28°$). Curves H_{55-41} and S_{55-41} in Fig. 7 represent respectively the intensity of the penetrating radiation and of the radiation absorbed in 12 cm of lead originating from primaries in the energy range 1 to 4 GeV. Both components have an absorption mean free path in air of approximately 90 g/cm^2 at pressures higher than 7 cm Hg and level off at lower pressures. Electrons cannot be present in

large numbers as they would produce a strong transition effect close to the top of the atmosphere and would not contribute to the penetrating component. μ-mesons would be absorbed in air less rapidly than indicated by H_{55-41}. Hence, it is concluded that primary and secondary nucleons are mainly responsible for the two components.

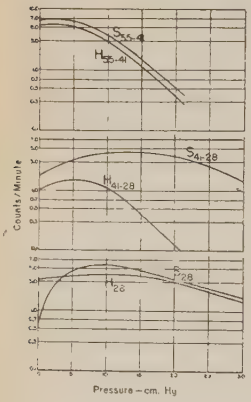

Fig. 7. – Altitude dependence of the intensity of the penetrating radiation (H) and of the radiation absorbed in 12 cm of lead (S) originating from primaries in the energy range: 1 to 4 GeV (cutoff energy at $\lambda = 55°$ and 41°), 4 to 8 GeV ($\lambda = 41°$ and 28°) and > 8 GeV ($\lambda = 28°$).

This interpretation is given added support by the similarity in the altitude dependence of this radiation to the altitude dependence of nuclear disintegrations, known to be produced by the nucleonic component, as observed with photographic emulsions ([29]) and ionization chambers ([30]).

A small contribution to the soft and hard component from electrons and μ-mesons respectively cannot be ruled out by this experiment.

Curves H_{41-28} and S_{41-28} in Fig. 7 represent the penetrating and the soft components originating from primaries in the energy range of 4 to 8 GeV. The increase by a factor of 2 in the intensity of the soft component from 1.5 to 12 cm Hg pressure indicates that primaries in the energy range of 4 to 8 GeV give rise to electronic cascades in the atmosphere. This effect can be explained by noting that the decay of a single neutral meson of an energy of a few GeV can originate an electron shower of moderate multiplicity. The low intensity of the penetrating component is due, at least partially, to the fact that charged mesons produced in the primary interaction decay into μ-mesons and do not give rise to subsequent nucleonic cascades.

Curves H_{28} and S_{28} in Fig. 7 represent respectively the penetrating and the soft component originating from primaries of energy greater than 8 GeV Both components show a strong transition effect with a maximum intensity at approximately 10 cm Hg pressure. From 1.5 to 10 cm Hg pressure the soft component increased by a factor of 3.2 and the hard component by 1.2. This strong multiplication in the first few mean free paths in the atmosphere indicates that primaries having an average energy of approximately 15 GeV can produce, in their interaction with air nuclei, nucleonic and mesonic cascades of rather high multiplicity. The fact that the soft and hard components reach

([29]) J. J. LORD: *Phys. Rev.*, **81**, 901 (1951).
([30]) A. N. WHITE: *Phys. Rev.*, **82**, 204 (1951).

maximum intensity at the same atmospheric depth is an added indication that both must have a common origin, namely those nuclear interactions which give rise to neutral and charged mesons.

4. – Production of multiple events in Hydrogen.

4·1. – *Design of the Apparatus.* – In order to study multiple events produced by cosmic ray particles in a liquid Hydrogen target, a counter experiment was carried out at an altitude of 90 000 ft.

The spherical copper Dewar container used to store the liquid Hydrogen had a capacity of 15 liters. The inside wall of the Dewar was 0.07 cm in thickness and the outside wall 0.08 cm . It was not considered avdisable to sorround the Hydrogen with a liquid Nitrogen jacket in order to avoid placing an additional thickness of heavier material above the counter trays registering the multiple events expected to originate in the Hydrogen. The rate of evaporation of liquid Hydrogen was measured in the laboratory at atmospheric pressure and found to average approximately 205 cm^3 per hour. No appreciable change in evaporation rate was noticed when the neck of the Dewar was tilted at an angle of 45° with respect to the vertical direction or when the Dewar was subjected to shocks and vibrations.

Solidification of the Hydrogen at the low atmospheric pressures reached in the stratosphere would result in a considerable loss of Hydrogen due to the heat of fusion released in the process of solidification. In order to prevent this event from occurring, the pressure inside the container was mantained approximately 5 lbs above the pressure of the sorrounding air during the flight. The Dewar and the accessory equipment are shown schematically in Fig. 8. The valves V, used to pressurize the liquid Hydrogen, were sealed with rubber gaskets (O rings seal). Two adjustable screws which tightened the helical steel springs of the valves made it possible to vary the pressure difference between the inside of the container and the outside atmosphere. A pressure gauge M connected permanently to the system served as a visual check on their operation on the ground. The valves were also used to prevent atmospheric Oxygen from condensing inside the container, thus avoiding the danger of forming an explosive mixture.

The liquid Hydrogen was ejected from the container while the balloon was floating at an altitude of 90 000 ft. This was necessary in order to obtain, by a difference measurement, the effect of Hydrogen on the type of events observed, also as safety precaution in case the equipment was damaged in landing. The method used to eject the liquid is shown in Fig. 8. A monel metal tubing T reaching to the bottom of the Dewar was sealed by means of two glass stems G. These were shattered at the time of ejection by means

of relays operated by alarm clocks. The liquid Hydrogen was then forced out of the gondola through the tubing T by the pressure mantained above the liquid.

Fig. 9*a* shows the front view and Fig. 9*b* the side view of the counter arrangement. Coincidences of the type *ABCD* or *EFGH* activated a master pulse. Any of the counters in the equipment, including counters *A*, *B*, *C*, *D*, *E*, *F*, *G* and *H* which were activated at the time of the occurrence of the master pulse flashed individual neon lamps (hodoscope).

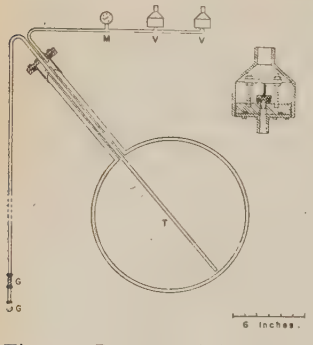

Fig. 8. – Dewar container used in the Hydrogen experiment.

A 35 mm camera was used to record the data obtained during the flight. The film was driven at a constant speed by an electric motor. The vertical stack of neon bulbs placed perpendicular to the motion of the film and collimated by a narrow slit recorded coincidences. Incandescent lights marked fiducial lines and were used to give information as to the position of relays. Every 10 minutes a lamp was flashed and the film recorded the time, the temperature of the equipment and the atmospheric pressure at the time of exposure. Two mercury U-tubes measured the pressure below 12 cm Hg. Pressure data were also obtained with a barograph and with an Olland cycle type barometer which transmitted readings to the ground station.

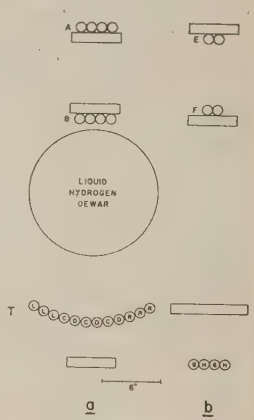

Fig. 9. – Schematic diagram of apparatus used for the study of multiple events originating in liquid Hydrogen. *a*, front view; *b*, side view.

Fig. 10 is a schematic drawing of a portion of the photographic record obtained.

The data that will be presented was obtained in flight IV (see Table I)

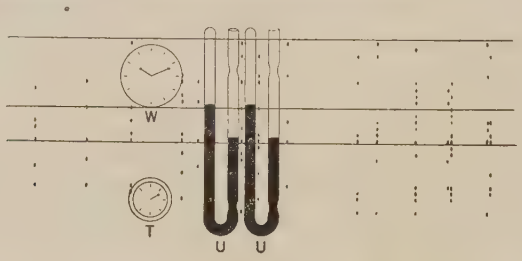

Fig. 10. – Drawing of a portion of the photographic record obtained in the Hydrogen experiment.

launched from Chicago on September 6, 1950 in which the balloon floated for several hours at an atmospheric pressure of 1.4 cm Hg, constant to within 0.1 cm Hg. During the first 130 minutes of flight at altitude an average of approximately 1.6 g/cm² of liquid Hydrogen was interposed between the counters. The Hydrogen was then ejected and data obtained during 110 minutes with an average of 0.2 g/cm² of liquid Hydrogen remaining in the Dewar flask. Fig. 11 gives the estimated amount of Hydrogen present in the counter arrangement during the flight. On recovery of the equipment, within a few minutes of the landing, the Dewar was promptly examined and found to contain only a few cm³ of liquid Hydrogen. Both glass seals were shattered and the relays, which left a mark on the photographic record, had acted at the correct time. The Dewar was tested and the rate of evaporation was found to be unchanged.

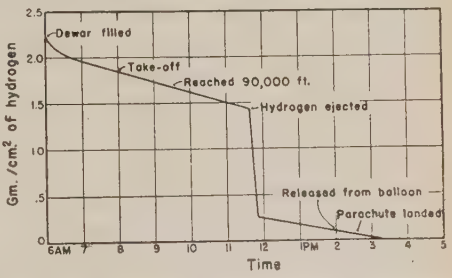

Fig. 11. – Amount of liquid Hydrogen (g/cm²) present in Dewar during the flight of September 6, 1950.

Due to the high intensity of the cosmic radiation close to the top of the atmosphere, a certain number of accidental coincidences were recorded. To eliminate such spurious events only those counts were analyzed in which at least one counter was discharged in the *GH* tray (see Fig. 9) in addition to two or more counters in tray *T*. This requirement reduces the number of accidental coincidences to a negligible fraction of the total counting rate.

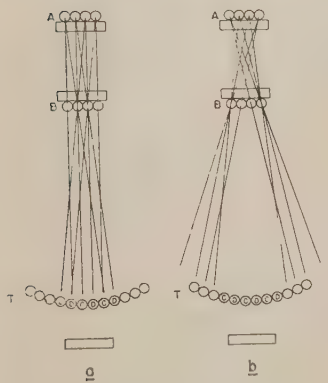

Fig. 12. – Type of events detected in the Hydrogen experiment.

4·2. – *Experimental results.* – All coincidences registered by the apparatus may be divided into two groups according to whether (1) only one counter or (2) several counters were activated in any one of the four trays *A*, *B*, *E* and *F* above the Hydrogen (see Fig. 9). Coincidences of type (1) are assumed to be due to a single incident particle interacting in the liquid Hydrogen or in the walls of the Dewar. Those of type (2) are of a more complicated nature and will be described in a later publication.

Events (1) were further subdivided depending on the direction of the incident particle as determined by which counters were traversed in trays *A* and *B*. Fig. 12*a* and *b* indicates how this choice was made. Events *a* are those in which a particle was incident on the equipment from the vertical, or nearly vertical, direction so as to have a high probability of traversing counters *C* or *D*. Events *b* are caused by particles incident on the apparatus at a much less favorable angle.

Table VIII gives the frequency of the events of type 1*a* and 1*b* obtained during 130 minutes of flight at 90 000 ft with liquid Hydrogen, and during 110 minutes after the ejection of the Hydrogen. The frequency of events of type 1*a* in which 2 or 3 counters were activated in tray *T* decreases noticeably after the ejection of the Hydrogen. No change is apparent in events of higher multiplicity. Events of type 1*b* do not show any change in frequency after the ejection of the Hydrogen and can be attributed to nuclear disintegrations of high multiplicity and wide angular spread originating in the heavy material of the equipment. From geometrical considerations the counter combinations corresponding to events of type 1*a* and 1*b* should have approximately the same counting rate. However only 19% of the events detected were of type *b*. This indicated that secondary particles are collimated in the direction of the incident particle.

TABLE VIII. – *Frequency of Multiple Events Observed with the Hydrogen Equipment.*

Type of event	Number of counters activated in tray *T*	Frequency of events with Hydrogen (cnts/h)	Frequency of events without Hydrogen (cnts/h)
1*a*	$\geqslant 2$	43 ± 5	33 ± 4
1*a*	$\geqslant 3$	24 ± 3	12 ± 3
1*a*	$\geqslant 4$	15 ± 3	17 ± 3
1*b*	$\geqslant 2$	18 ± 3	17 ± 3

The location of the counters activated in the tray below the Hydrogen can give some information on the angular distribution of secondary particles. Figs. 13*a* and 13*b* are histograms of the frequency of all events of type 1*a* originating in the walls of the Dewar and in liquid Hydrogen respectively, plotted as a function of their total angular width. This width is assumed to correspond to the angular separation, as seen from the geometrical center of the Dewar, of the two farthest counters activated in tray *T* (see Fig. 9). Fig. 13*a*, which refers to the number of events originating in the walls of the Dewar, has a sharp maximum at an angular width of approximately 4°, an effect that can be attributed to the break up of α-particles. The remaining

events show a rather uniform particle distribution over the area of counter tray T and are attributed to stars in the copper walls of the Dewar. Events originating in the Hydrogen have a much narrower angular spread (see Fig. 13*b*),

A selection of those coincidences in which at least three counters were activated in tray T, eliminates the possibility that some of the events recorded

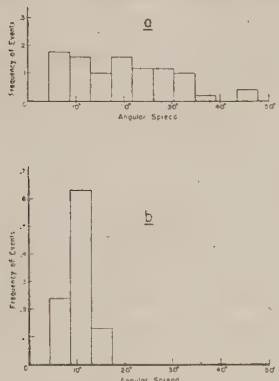

Fig. 13. – Angular distribution of events of type 1*a* originating in: *a*, the walls of the Dewar flask; *b*, the liquid Hydrogen.

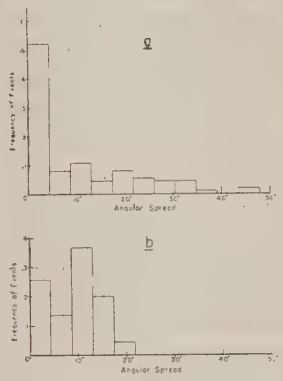

Fig. 14. - Angular distribution of events of type 1*a* in which 3 or more counters were activated in tray T originating in: *a*, the walls of the Dewar flask; *b*, the liquid Hydrogen.

may have been due to knock on electrons, break up of α-particles, elastic collisions and other interactions giving rise to events consisting of two secondary particles only. Figs. 14*a* and 14*b* are histograms of the frequency of events of type 1*a* in which three or more counters were activated in counter tray T, originating in the walls of the Dewar and in the liquid Hydrogen respectively, plotted as a function of their total angular width. Fig. 14*a* shows that events originating in the walls of the Dewar are isotropically distributed over the area of counter tray T. The events of an angular spread of more than 35° are detected less efficiently by the counter arrangement used. The absence of events of an angular width of less than 4° results from the requirment that three counters be discharged in counter tray T. The finite size of the counters places a lower limit on the minimum angular spread observed. Fig. 14*b* shows that events originating in Hydrogen have an angular spread of only 15° indicating that low energy interactions cannot have contributed significantly to the counting rate. This is in agreement with the fact that real stars cannot be produced in proton-proton collisions, and with the evidence obtained in cloud chambers where it is found that this degree of collimation is found only in events of very high energy.

The fact that the number of events in which two or three counters were discharged in tray T is approximately equal (see Table VIII), indicates that the multiplicity of the events observed to originate in liquid Hydrogen is high. From this it is estimated that showers in which three or more counters were activated must have consisted of 6 or more particles. It follows that in proton-proton collisions a minimum of 4 mesons must have been produced, or, in the collisions of α-particles with Hydrogen nuclei a minimum of two mesons, in addition to the nucleons resulting from the break up of the α-particles.

The multiplicity of meson production is known to be a slowly varying function of the energy of the interacting particles. Since α-particles represent only a small fraction of the primary cosmic ray flux ($\sim 15\%$) and since their average energy per nucleon is considerably lower than the average energy of the proton component, the observed counting rate can be attributed predominantly to multiple meson production in proton-proton collisions. It is estimated that not more than 20% of the observed counting rate is due to the interaction of α-particles and heavier nuclei with the target protons.

From a careful analysis of the counter geometry and from the knowledge of the amount of liquid Hydrogen present in the counter arrangement, the flux of the radiation giving rise to multiple events in Hydrogen can be computed. Table IX gives the flux of primary protons required to explain the observed counting rate assuming the following values for the cross-section of multiple meson production in proton-proton collisions: *a*) cross-sectional area of a proton ($\pi r_0^2 = 6.15 \cdot 10^{-26}$ cm^2, where r_0 = range of nuclear forces = $= 1.4 \cdot 10^{-13}$ cm; *b*) two times the geometrical area; and *c*) four times the geometrical area. From the energy spectrum obtained in Section 3·2, the minimum energy corresponding to each value of the flux is given in Table IX.

TABLE IX.

Collision cross-section (in units of $\pi r_0^2 = 6.15 \cdot 10^{-26}$)	Proton flux (per cm^2/sterad/s)	Minimum proton energy (GeV)
1	0.011	50
2	0.0055	130
4	0.0028	320

The table clearly shows that the assumption of a cross-section much higher than geometrical leads to very high energies of the incident protons. From data obtained in photographic emulsions it is known that meson showers at these high energies would have a prohibitively small angular spread and could not be detected efficiently by the counter arrangement. It is therefore con-

cluded that the observed counts in Hydrogen are consistent with a cross-section between 1 and 2 times the nuclear area of a proton. This in turn corresponds to a proton energy of 50÷100 GeV.

It appears, therefore, that the production of 4 or more charged mesons in proton-proton collisions occurs with high probability only at incident proton energies of the order of 50 to 100 GeV. This energy is considerably higher than the energy predicted by the older theories on multiple meson production. It is, however, consistent with the result of the statistical theory of E. FERMI ([17]) and with some observations of very high energy stars which have been found in nuclear emulsions ([1,14]).

5. – Production of multiple events in lead.

The counter apparatus CT_1 (Fig. 1) was designed to register the production by ionizing radiation of penetrating events in a lead block 12 cm in thickness. The counting rate of the coincidence sets *BCDE*, *BCDF* and *BCDG* discharged simultaneously is given in Fig. 15. Curve *A* was obtained in flight II at $\lambda = 55°$ (see Table I) and curve *B* in flight I at $\lambda = 28°$. Such events require the tripping of all three counters below the lead block so that a minimum of three penetrating particles must be involved in the process. Events of this type are due to penetrating showers of moderate energy originating in the lead since the contribution of air showers is found to be small in such high order coincidences close to the top of the atmosphere.

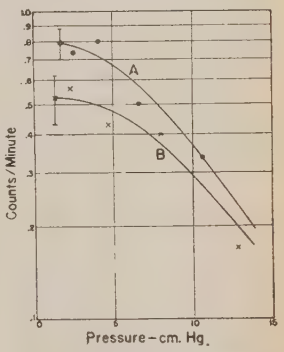

Fig. 15. – Altitude dependence of penetrating showers originating in lead at: *A*, $\lambda = 55°$; *B*, $\lambda = 28°$.

Curve *A* in Fig. 15 exhibits a plateau at pressures lower than 4 cm Hg, whereas curve *B* begins to level off at a pressure of 10 cm Hg. At pressures higher than 10 cm Hg, both curves drop rapidly. Assuming an exponential absorption for the radiation producing penetrating showers, one obtains results at the two latitudes consistent with an absorption mean free path of about 120 g/cm². The altitude dependence of penetrating showers has been measured up to 20 cm Hg pressure by other authors ([31,32]) who have obtained very nearly the same absorption mean free path. From Fig. 15 one

([31]) T. G. WALSH and O. PICCIONI: *Phys. Rev.*, **80**, 619 (1950).
([32]) A. J. MCMAHON, B. ROSSI and W. F. BURDITT: *Phys. Rev.*, **80**, 157 (1950).

sees that penetrating showers exhibit a relatively small latitude effect between $\lambda = 55°$ and $\lambda = 28°$. The largest latitude effect occurs at the maximum altitude reached (1.5 cm Hg pressure) and amounts to 1.5 ± 0.37 as compared to 2.9 ± 0.2 for the hard component and 4.1 ± 0.1 for the total radiation. The small latitude effect of penetrating showers as measured here up to the highest altitudes shows that at $\lambda = 55°$ they originate from a radiation 67% of which is produced by primary protons of energy greater than 8 GeV or primary heavy nuclei of energy greater than 3.5 GeV per nucleon (cut-off energies at 28° geomagnetic latitude).

Since at high altitude one can assume that most of the penetrating showers are due to nucleons, the plateaus occurring in these curves must be attributed to the presence of successive nuclear processes developing in the air. The plateau at $\lambda = 28°$ extends to considerably lower altitudes than at $\lambda = 55°$. This effect strongly indicates that, due to the higher average primary energy at the lower latitude, the chains of nucleonic cascades are of considerably greater extension in the atmosphere than the corresponding ones at $\lambda = 55°$.

The fact that even at $\lambda = 28°$ only a small fraction of the penetrating radiation gives rise to events capable of triggering the three counters *E*, *F* and *G* below the lead block indicates that particles with an average energy of approximately 20 GeV do not produce events of sufficient multiplicity in their interaction in lead to be recorded with high efficiency by the coincidence arrangement.

6. – Summary of results.

A number of counter experiments carried out close to the top of the atmosphere have given a considerable amount of information on the nature of high energy nuclear interactions. A summary of the results obtained in these experiments is given below.

1) The intensity of the total and hard component of the cosmic radiation was measured as a function of altitude at $\lambda = 55°$, 41° and 28°. At these three latitudes both components show a definite maximum which occurs at approximately 6, 8 and 10 cm Hg pressure, respectively.

2) The various components of the cosmic radiation, as measured through several thicknesses of lead at $\lambda = 55°$, 41° and 28°, do not extrapolate to a common point at the top of the atmosphere. This effect is most pronounced at high latitudes. Fig. 16 gives the absorption of the radiation in lead at $\lambda = 41°$ for atmospheric pressures of 0, 2 and 8 cm Hg. The primary flux is absorbed in lead with a mean free path of 300 g/cm². From this result the following conclusions can be drawn: *a*) the contribution of particles incident from the bottom of the apparatus must be small; *b*) the number of electrons present at the top of the atmosphere cannot be large, since they

would be rapidly absorbed in lead; *c*) secondary nucleons with an energy sufficiently low to have their path curved by the magnetic field of the earth so as to approach the equipment from the vertical direction, would be absorbed in a few centimeters of lead and therefore cannot be present in large numbers at the top of the atmosphere; *d*) the value obtained for the absorption mean free path of the primary cosmic radiation is approximately equal to twice the nuclear mean free path and is in good agreement with results of other investigators on the absorption of high-energy nucleons in lead.

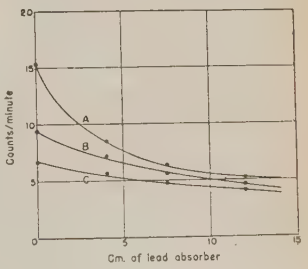

Fig. 16. - Absorption of the cosmic radiation in lead at $\lambda = 41°$ measured at an atmospheric pressure of: *A*, 8 cm Hg; *B*, 2 cm Hg; *C*, 0 cm Hg.

At 8 cm Hg pressure (corresponding to the maximum intensity of the total radiation at $\lambda = 41°$) the steep slope in the absorption curve through the first few centimeters of lead is interpreted as due to the presence of the electronic component.

3) The latitude effect of the components of the cosmic radiation was obtained for several atmospheric depths and is found to have its highest value for the total component at the top of the atmosphere.

4) The momentum spectrum of the primary radiation was obtained by extrapolating the vertical intensity of the total component to 0 pressure. This spectrum can be well represented by a power law of the following type:

$$N\left(> \frac{pc}{Ze}\right) = 0.48 \left(\frac{pc}{Ze}\right)^{-1.0} .$$

5) The altitude dependence of the hard and soft components originating from primaries of energy in the range 1 to 4 GeV is very similar to the altitude dependence of the nucleonic component. It is concluded that in this energy range the secondary radiation is predominantly nucleonic in character and that meson production does not occur with high probability.

6) Meson production becomes important for energies of the order of 4 to 8 GeV. This is indicated by the strong multiplication of the soft component originating from primaries in this energy range. In addition, the low intensity of the hard component shows that mesons are mainly produced singly.

7) Both the soft and hard components produced by primaries of energy higher than 8 GeV show a definite transition effect in the atmosphere. A pronounced maximum is found at 10 cm Hg pressure. At these high energies the production of more than one meson in the interaction of a primary particle with an air nucleus becomes important. As discussed in Section **4**, much

higher energies are needed to produce several mesons in a single nucleon-nucleon collision. Therefore it seems that to give rise to the observed effect, several successive nucleon-nucleon collisions or meson-nucleon collisions must occur within a single nucleus, each collision producing additional mesons. The fact that at latitudes of $\lambda = 28°$ and 41° all components have their maximum intensity at an atmospheric pressure corresponding to about two nuclear mean free paths from the top of the atmosphere, is strong evidence that they originate mostly in primary nuclear interactions where it is known that the production of charged and neutral mesons is predominant.

8) A counter experiment was carried out at an altitude of 90 000 ft to study the production of mesons in a liquid Hydrogen target. The Hydrogen was removed while the apparatus was floating at this altitude and the background counting rate of the equipment was obtained. A significant difference in the frequency of certain types of events with and without Hydrogen was found and was interpreted as due to interactions of cosmic ray particles with Hydrogen nuclei. Events originating in Hydrogen have a narrow angular spread in contrast with the wide angular distribution of events originating in the walls of the Dewar container. An analysis of the events shows that they must be due predominantly to primary protons giving rise to multiple meson production in collisions with Hydrogen nuclei. It is estimated that primary protons of an average energy of approximately 50 to 100 GeV interact in Hydrogen with a cross-section approximately equal to the cross-sectional area of a proton ($6.15 \cdot 10^{-26}$ cm^2) producing 4 or more charged mesons.

9) The frequency of penetrating showers originating in a lead block of 12 cm thickness was measured at $\lambda = 55°$ and 28°. The radiation producing penetrating showers is found to have an absorption coefficient in air of approximately 120 g/cm^2. For pressures lower than 10 cm Hg at $\lambda = 28°$ and lower than 5 cm Hg at $\lambda = 55°$, both curves level off. At $\lambda = 55°$ and 28° one obtains, for events of this kind, a latitude effect of 1.5 as compared to a value of 2.9 for the latitude effect of the hard component and 4.1 for the total component as measured at a pressure of 1.5 cm Hg.

The authors would like to express their thanks to Professor EARL LONG of the Institute for the Study of Metals of the University of Chicago for furnishing the liquid Hydrogen and for his assistance in the design and preparation of the Dewar container. The cooperation of the Office of Naval Research and of the staff of the General Mills Company in arranging the balloon flights and in making every effort to make these experiments successful is deeply appreciated. Thanks are also due to Mr. RAYMOND FOSTER and Mr. JOHN BJORKLAND for their invaluable help in the construction and operation of the equipment.

RIASSUNTO (*)

Una indagine sulla dipendenza dall'altitudine e la latitudine dei vari componenti della radiazione cosmica fornisce informazioni sulle interazioni nucleari di particelle cosmiche coinvolgenti elevate energie che hanno luogo vicino al limite dell'atmosfera. A mezzo di palloni di materia plastica si sono mandati dei telescopi di contatori all'altezza massima di 29 000 m (94 000 ft). Sono state rilevate curve dell'intensità in funzione della pressione alla latitudine geomagnetica $\lambda = 55°$, 41° e 28° per la radiazione cosmica totale e per i suoi componenti capaci di traversare 4, 7,5 e 12 cm di Piombo. Lo spettro d'energia delle particelle primarie della radiazione cosmica è stato ottenuto per estrapolazione dell'intensità della radiazione totale al limite dell'atmosfera. Lo spettro integrale della quantità di moto della radiazione primaria totale è data da $N(> pc/Ze) = 0{,}48(pc/Ze)^{-1{,}0}$. Sottraendo il contributo noto delle particelle α primarie e dei nuclei più pesanti, lo spettro dei protoni primari diventa $P(> pc/e) = 0{,}43(pc/e)^{-1{,}0}$. I risultati indicano che la radiazione derivante dai primari nella gamma d'energia tra 1 a 4 GeV (energie di taglio a $\lambda = 55°$ e 41°) è prevalentemente di natura nucleonica. L'assenza di una componente elettronica può essere spiegata assumendo che vicino al limite dell'atmosfera gli elettroni hanno origine prevalentemente dal decadimento di mesoni neutri e che a questi livelli energetici la probabilità di generazione dei mesoni è assai piccola. In netto contrasto con questo comportamento, la componente molle prodotta dai primari nella gamma da 4 a 8 GeV (taglio a $\lambda = 41°$ e 28°) si moltiplica rapidamente nell'atmosfera. Questo forte effetto di transizione nell'aria con un massimo a circa 10 cm Hg di pressione è caratteristico degli sciami di elettroni. Si conclude che la probabilità di produzione dei mesoni neutri isolati raggiunge quasi il valore di saturazione per energie della radiazione primaria comprese fra 4 e 8 GeV. Ad energie maggiori di 8 GeV questo effetto è ancora maggiormente pronunciato a causa della produzione plurima di mesoni. Onde studiare la produzione di mesoni nell'interazione di particelle della radiazione cosmica con un bersaglio di Idrogeno liquido è stato eseguito un esperimento con contatori all'altezza di 27 500 m (90 000 ft). Durante la prima metà dell'esperimento una media di 1,6 g/cm² di Idrogeno fu interposto fra i contatori. Poi l'Idrogeno fu evacuato e furono raccolti i dati durante la seconda metà del volo in quota. Dalla ristretta distribuzione angolare degli eventi aventi origine nell'Idrogeno liquido (dispersione angolare totale $\sim 15°$), nettamente differente da quella degli eventi aventi origine nelle pareti del recipiente Dewar (dispersione angolare minima $\sim 50°$) si conclude che furono prodotti da particelle primarie di elevata energia. Si stima che gli eventi rilevati nell'Idrogeno risultarono prevalentemente (80%) dovuti all'interazione di protoni primari di energia media di 50 ÷ 100 GeV in cui furono prodotti un minimo di quattro mesoni. Sono stati studiati sciami penetranti in Piombo a $\lambda = 55°$ e 28°. Tra queste due latitudini, alla pressione di 1.5 cm Hg, il rapporto d'intensità della radiazione producente sciami penetranti è 1.5 in confronto di 2,9 per la componente dura e 4,1 per la radiazione totale.

(*) *Traduzione a cura della Redazione.*

Detection of Nuclear Interactions by Means of a Cloud Chamber containing a Crystal of Sodium Iodide.

G. SALVINI

Palmer Physical Laboratory, Princeton University - Princeton, N.J.

(ricevuto il 30 Luglio 1951)

Summary. — A cloud chamber with a proportional crystal inside was operated, in order to estabilish some properties of the cosmic ray nuclear events, whose study is complicated or impossible in cloud chambers triggered with Geiger-Müller counters, for the selection introduced in detecting the events. The apparatus is described, and the results obtained in sixty days at sea level are given, in regard to the mean free path of the shower particles in Carbon (108 g/cm²), and to the probability of production of the eletromagnetic component in high energy nucleon-nucleus collisions ($\sigma \sim 1/4$ of the geometrical).

---

1. – In the systematic study of nuclear interactions by means of cloud chambers some difficulties arise in attempting to make an unbiased selection of the events to be studied. The usual way of detecting nuclear events with Geiger-Müller trays above or below the cloud chamber introduces in particular an unknown selection of the nuclear events ([1,2]). It is evident for instance that this difficulty is particularly pronounced with respect to studies of:

— The electromagnetic component (neutral mesons) produced in nucleon-nucleus collisions at fairly high energy ([3]),

— Mean free path for nuclear interactions of the particles emitted in the nuclear events ([1,2,3]),

---

([1]) A. LOVATI, A. MURA, G. SALVINI and G. TAGLIAFERRI: *Nuovo Cimento*, **7**, 36 (1950) and bibl.; *Phys. Rev.*, **77**, 284 (1950).

([2]) G. SALVINI: *Nuovo Cimento*, **7**, 786 (1950).

([3]) B. FRETTER: *Phys. Rev.*, **76**, 511 (1949); A. LOVATI, A. MURA, G. SALVINI and G. TAGLIAFERRI: *Nuovo Cimento*, **7**, 943 (1950).

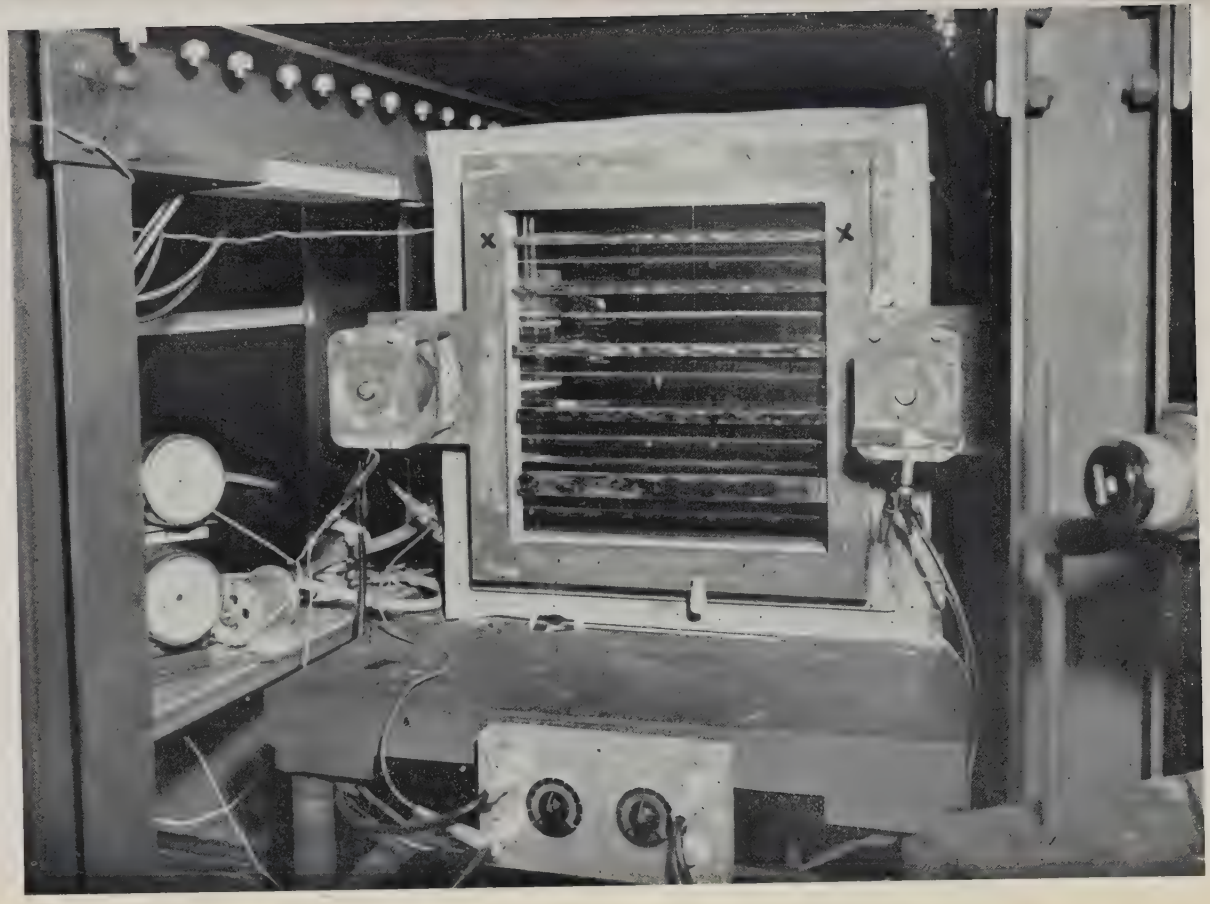

Fig. 1. – Photograph of cloud chamber containing NaI crystals and plates of Pb and C for study of mean free paths and meson production. The first plate ( ) contains the crystals. The two expansion valves appear on the sides.

A nuclear explosion in the crystal.

Nuclear interaction in the crystal, with a successive interaction in Pb (6th plate). The vertical line is a wire we put for calibration of the stereoscopy.

Nuclear explosion in the crystal with a successive interaction in C (5th plate).

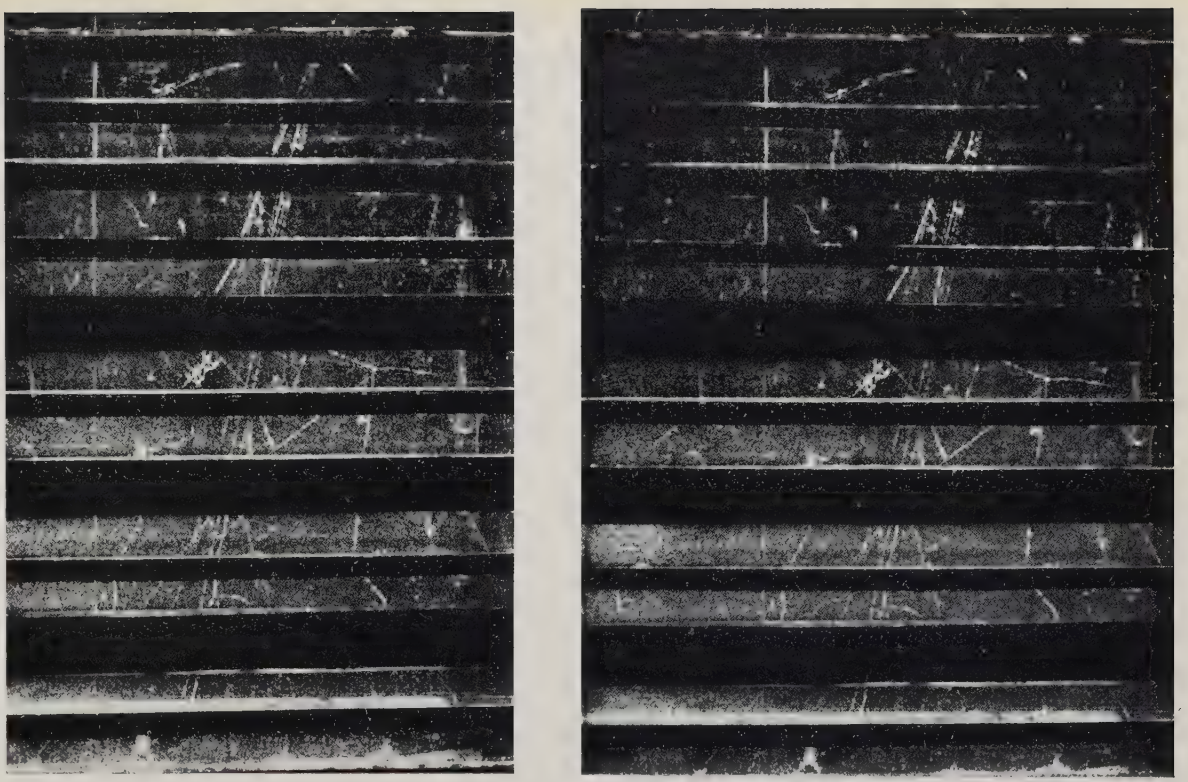

Nuclear explosion in the crystal with a successive interaction in C (7th plate). Five relativistic particles are emitted forward in the explosion in the crystal; no electromagnetic component was emitted.

— Frequency of occurrence of phenomena that may escape detection with other techniques, such as the measurement of the frequency of emission of the new heavy mesons in cosmic rays nuclear events (4), or the probability of proton-neutron exchanges in nuclear interactions or low energy exchanges generally (5).

In view of the interest in these interactions, an apparatus has been built to permit relatively unbiased selection of the events to be studied. An almost unbiased selection such as that obtained with nuclear plates would allow us to correlate in a more definite manner the results in the cloud chamber with the ones reached with the nuclear emulsion technique.

The technique used is to place a proportional scintillation crystal counter inside a cloud chamber. The cloud chamber is triggered by means of the signal from photomultipliers viewing the crystal, when that signal indicates that at least one heavily ionizing particle has resulted from an interaction in the crystal. In this way, selection is made on the basis of the energy of the heavily ionizing particles resulting from the interaction, regardless of the detailed behaviour of the secondary particles of higher energy, so that the bias is no more severe in regard to protons of fairly high energy (100 MeV up) and to mesons, than the bias usually introduced in the nuclear emulsion technique.

2. – Apparatus.

The cloud chamber is a rear illuminated type, shown in fig. 1, not very different from other types already reported in the literature (6), in particular quite close, apart from the modifications in some details, due to the enlarged dimensions, to the type employed by R. RAU. The illuminated dimensions are $46 \times 46 \times 20$ cm.

The requirements of the scintillation crystals inside the cloud chamber are dictated by the decision to observe all events that give rise to the emission, inside the crystal material, of at least one heavily ionizing particle. This selection can be rather large, including for example all of the nuclear events usually observed in the nuclear emulsions. In order that this criterion result in an unbiased selection on the basis of the energy transferred to « evaporation » (or slow knock on) particles, it is necessary to employ a crystal in which there is good proportionality between the quantity of fluorescent light emitted

(4) A. J. SERIFF, R. B. LEIGHTON, C. HSIAO, E. W. COWAN and C. D. ANDERSON: *Phys. Rev.*, **78**, 290 (1950).

(5) J. TINLOT and B. GREGORY: *Phys. Rev.*, **81**, 667 and 675 (1951).

(6) R. RAU: *Princeton cosmic ray group, technical report n. 4*; M. B. GOTTLIEB: *Phys. Rev.*, **82**, 349 (1951).

and the energy loss of the ionizing particles, relatively independent of the latter's velocity and charge. This requirement evidently rules out the organic liquids and crystals known at present, and leads to a choice of NaI crystals, which have been studied extensively in this laboratory by HOFSTADTER (7) and are known to be proportional in their energy response to a satisfactory degree in the energy region of interest.

In order to avoid taking pictures that are not of interest in the first studies, it is necessary to bias against observing the simultaneous passage through the crystal of greater than a certain number of relativistic particles (say 2 or 3). This condition is easily achieved by making the NaI crystal thin enough, but

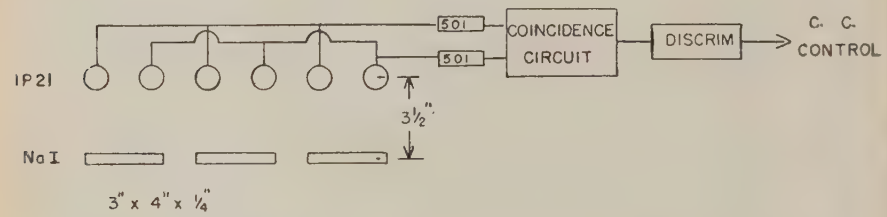

Fig. 2. – Crystal and photomultiplier disposition, and block diagram of circuitry.

this in turn restricts the possible means of transmitting the light from the crystals to the photomultipliers.

Accordingly, a preliminary study was made by means of Geiger counters, crystals and photomultipliers to determine the effectiveness of various dispositions for the detection of different energy losses (from several MeV up) within reasonable limits of statistical fluctuations, arising from the fluctuations of the electrons in the photomultipliers. These experiments led to the configuration shown in fig. 2. The three crystals are each $3'' \times 4'' \times 1/4''$ thick, and are viewed by six photomultipliers arranged in two groups of three in parallel. The photomultipliers are 1P 21's of better than average characteristics, but not critically so. Each of these two groups of photomultipliers leads to a fast amplifier (rise time ~ 0.2 μs), and thence to a two-fold coincidence circuit. (The coincidence circuits in use have 5 additional coincidence channels and one anticoincidence channel available, so that alternate selection schemes, mentioned below, may be used where desireable). The resolving time of the coincidence circuit is ~ 1 μs. The output of the coincidence circuit leads to the discriminator, where the energy selection is made. With this disposition

(7) R. HOFSTADTER: *Phys. Rev.*, **75**, 796 (1949). See also G. REYNOLDS and F. HARRISON: *Phys. Rev.*, **76**, 169 (1949); W. FRANZEN, R. SHERR and R. PEELLE: *Phys. Rev.*, **79**, 742 (1950).

it has proved possible to detect all events that dissipate more than 2 MeV in the crystal. It is thus possible to bias in such a way that at least 1, or 2, etc., relativistic particles are required to trigger. For the experiments described here, two different biases were set in two different periods: the first so that 6 MeV energy loss in the crystal was necessary for the triggering process, the second so that 12 MeV were necessary: no difference in the statistics of the relativistic nuclear events was noticed. These figures, indicated by the Geiger counter experiments, have been confirmed by direct observation with the cloud chamber.

The general assembly is shown in fig. 3. The NaI crystals are mounted in the top plate of the cloud chamber. The photomultipliers are mounted

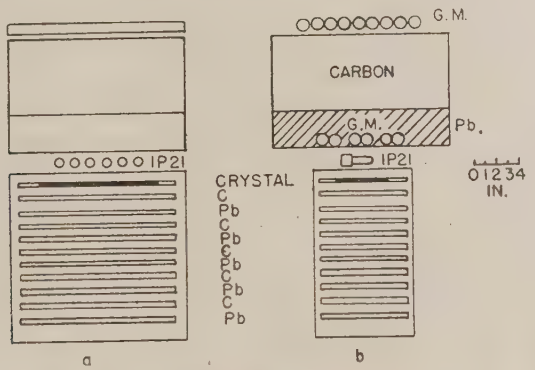

Fig. 3. - Front and side view of general assembly of cloud chamber, crystals and plates.

above outside the cloud chamber and view the crystals through a suitable glass window 1/4″ thick in the top of the chamber. The crystals are backed with aluminium foil sealed to a glass front with low vapor pressure wax in order to protect the NaI from the atmosphere of the chamber.

The control system is so arranged that the chamber may be triggered by 1) crystals alone 2) Geiger counters plus crystals or 3) Geiger counters alone. The control with the Geiger counters alone (fig. 3) was mainly used for comparison with the results with the crystals. The Geiger counter plus crystal control was prepared for studying the events produced by the protons.

The apparatus was operated for sixty days at sea level. We report here the results obtained on two lines of investigation:

---

(8) A. Lovati, A. Mura, C. Succi and G. Tagliaferri: *Nuovo Cimento*. 8. 271 (1951) and bibl.

— The mean free path in Carbon of the relativistic secondaries of nuclear interactions (80% of events selected by crystal alone 20% by a fourfold Geiger counter telescope above the cloud chamber);

— The cross section for production of the electromagnetic component in nucleon-nucleus collisions of high energy (all events selected by crystal alone).

3. – Mean free path in Carbon.

The mean free path of relativistic particles (not electrons) emitted in high energy nuclear interactions has been studied by many authors ([1,3,8,9]) using cloud chamber and nuclear emulsion techniques. In nuclear emulsions the mean free path is that for a nucleus of average mass around 80. In cloud chambers it is possible to know the atomic weight involved but as several authors have pointed out ([1,2]) selection of cloud chamber events by Geiger counters may influence the result: for example because of the fact that the probability of detecting a nuclear event with successive interactions is greater than that for an event in which the shower particles do not interact. Control by crystals alone is practically free of this bias.

In this experiment the cloud chamber contained alternated plates of Carbon (4 plates for a total of 22 g/cm²) and Lead (5 plates for a total of 30 g/cm²) below the Aluminum plate on the top, containing the crystals. The mean free path for nuclear interaction was measured for the relativistic particles emitted from nuclear explosions that occurred either in the crystal or in the material above the cloud chamber (fig. 3).

We consider as nuclear interactions of the relativistic particles in Carbon not only the nuclear trasmutations (stars and penetrating showers) involving heavy and (or) penetrating particles, but also scatterings greater than 10 degrees, and the disappearence of a relativistic penetrating particle in a Carbon plate in a well illuminated region of the cloud chamber (a careful use of the stereoscopy and discussion of the possible residual range in regard to the ionization losses made us quite sure that these last disappearences were due to nuclear interactions). The procedure was to follow all the relativistic penetrating particles emitted in the nuclear explosion from the crystal and traversing the Carbon plates, and estimating the mean free path from the ratio of g/cm² of Carbon traversed to the number of observed nuclear interactions in the Carbon. Of a total of 2270 g/cm² traversed, 21 nuclear interactions were observed, a large percentage being weak interactions. The mean free path of these particles in Carbon is thus:

$$2270/21 = 108 \pm 25\% \text{ g/cm}^2 .$$

([9]) U. Camerini, P. H. Fowler, W. O. Lock and H. Muirhead: *Phil. Mag.*, **41**, 413 (1950).

This result can be compared with other published results for the mean free path of the shower particles in the following table:

Material	Mean free path (g/cm^2)	Authors
Pb	170	TINLOT and GREGORY: *Phys. Rev.*, **81**, 667, 675 (1951)
Pb	200	LOVATI, MURA, SUCCI and TAGLIAFERRI: *Nuovo Cimento*, **8**, 271 (1951)
Au	230	A. J. HARTZLER: *Phys. Rev.*, **82**, 359 (1951).
Al	164	TINLOT and GREGORY: loco citato.
C	237	GREEN (upper limit): *Phys. Rev.*, **80**, 832 (1950).
C	108	Present experiment.

The results above apply to an unknown mixture of π-mesons and protons. However, in our case it is likely that the π-mesons are about 70% of the charged relativistic particles emitted in the nuclear interaction in the crystal, due to the fact that our detection is mainly based on the evaporation part like in the nuclear emulsion technique.

So, even though the mean free path for interaction of π-mesons alone can not be extracted from our data, it can be noted that the mean free path of the mixture is near that for the protons alone, suggesting that the mean free path for relativistic π-mesons may not be far different from the geometrical also in the light nuclei.

4. – Production cross section of the electromagnetic component in nucleon-nucleus collisions.

Using selection by crystals only, some preliminary measurements have been made on the production of the electromagnetic component. With our disposition the probability of detecting the nuclear events does not depend on the amount of penetrating particles or electromagnetic component, as usually in cloud chambers controlled with Geiger Müller counters.

If we accept, on basis of the work of the Bristol group ([10]), the hypothesis that this component arises from the decay of neutral mesons, then this cross section can be taken as the production cross section for neutral mesons, and is more certain than the corresponding cross section for the production of charged mesons, since in the later case there is uncertainty introduced because of proton emission in the region beyond one GeV.

([10]) A. C. CARLSON, J. E. HOOPER and D. T. KING: *Phyl. Mag.*, **41**, 701 (1950).

The electromagnetic component was observed by us by means of the pair production and cascade multiplication in the lead plates (and to a lesser extent in the Carbon plates) below the crystals in the cloud chamber. The probability that both of the two photons escape materialization and observation in the chamber depends on their energy and may be estimated. This probability of escaping detection is about 25% for neutral mesons of 200 MeV kinetic energy and approches zero rapidly as the energy increases.

In the longer range experiment now beginning at mountain altitude, classification of the nuclear events is on the basis of the numbers of grey and relativistic particles, the nature of the initiating particle, and the presence or absence of electromagnetic cores. If we apply this classification to the data observed so far at sea level we can say the following.

We considered together two kinds of nuclear events: (*a*) all the nuclear events containing at least two relativistic particles emitted, and representing an energy definitely larger than 1 GeV for the producing particle (as judged also by Coulomb scattering of the particles involved), and (*b*) the nuclear events with electromagnetic component and none or one penetrating particle coming out (only two events of this kind were observed).

Of 46 of these events we observed electromagnetic cores 12 times, and in each case no evidence for more than one neutral meson emitted. Therefore, the cross section for the production of neutral mesons in collisions of nucleons of > 1 GeV kinetic energy with a NaI « nucleus » is of the order of magnitude of 1/4 the geometrical cross section of the nucleus:

$$\sigma(n, p - \mathrm{NaI}) \sim (1/4)\sigma_{\mathrm{geo}} \sim (1/4)\pi r_0^2 A^{2/3} \sim 2.5 \cdot 10^{-25} \ \mathrm{cm}^2 .$$

In the estimation above we assumed that the total nucleon-nucleus cross section at high energies is about geometrical; $r_0 = 1.4 \cdot 10^{-13}$ cm; the nucleus equivalent to a « nucleus » of NaI (intermediate between Na and I) is a nucleus with atomic weight $A = 67$.

This value ($\sigma \sim 1/4$ geo) constitutes a superior limit for the cross section for emission of neutral mesons in the nucleon-nucleon collisions of energy > 1 GeV in the laboratory system.

It is expected that the data resulting from high altitude operation of the equipment described will replace the rather indirect information that is available at present with the nuclear emulsion technique ([10]) and the cloud chambers controlled with Geiger counters ([3,11]).

The author wishes to express his gratitude to Dr. G. T. Reynolds for experimental help and stimulating discussion, and to Mr. Young Kim for his collaboration.

([11]) A report of part of the results of this paper was given at the Washington meeting, 1951: G. Salvini and G. T. Reynolds: *Phys. Rev.*, **83**, 198 (1951).

RIASSUNTO

Nello studio delle interazioni nucleari della radiazione cosmica eseguito con camere di Wilson comandate da contatori di Geiger Müller il comando dei contatori introduce una selezione a priori degli eventi in istudio che rende particolarmente difficile lo studio delle proprietà delle particelle secondarie e della componente elettromagnetica (mesoni neutri) emesse. Per ovviare a queste difficoltà si è preparata una camera di Wilson comandata da contatori a cristallo fluorescente posti entro di essa, i quali rivelano le esplosioni nucleari in base alla «luce» emessa dalle particelle di evaporazione dell'interazione nucleare. Nella presente nota si riferiscono i particolari costruttivi dei rivelatori a scintillazione e della camera di Wilson. Si danno i risultati ottenuti in una serie di misure eseguite al livello del mare. Il cammino libero medio di interazione nucleare in C delle particelle secondarie delle esplosioni nucleari è risultato 108 $g/cm^2 \pm 25\%$. Si confronta questo risultato con quelli di altri autori in materiali diversi. La sezione d'urto per emissione di componente elettromagnetica (mesoni neutri) nell'urto di un nucleone veloce (energia maggiore di 1 GeV) contro un «nucleo» di NaI risulta dell'ordine di un quarto della sezione d'urto geometrica. Le misure continuano a 3 200 metri sul livello del mare.

LETTERE ALLA REDAZIONE

(La responsabilità scientifica degli scritti inscriti in questa rubrica è completamente lasciata dalla Direzione del periodico ai singoli autori)

Sui contatori a radiazione di Cerenkov.

P. Bassi

Istituto di Fisica dell'Università, Centro studio Ioni Veloci del C.N.R. - Padova

(ricevuto l'11 Settembre 1951)

Una particella carica che attraversa un mezzo di indice di rifrazione n con velocità $v > c/n$, vale a dire con velocità maggiore di quella della luce nel mezzo, emette un'onda luminosa. Questo fenomeno fu osservato per la prima volta da Cerenkov [1] e fu spiegato teoricamente da Frank e Tamm [2]. Più tardi Getting [3] e Dicke [4] hanno proposto di utilizzare la radiazione di Cerenkov per rivelare particelle cariche veloci; recentemente Jelley [5] è riuscito a contare singoli raggi cosmici con questo metodo.

Il metodo consente in linea di principio di misurare anche la velocità delle particelle, sia determinando l'angolo ϑ sotto cui viene emessa la luce, sia misurando le quantità W di energia luminosa prodotta (ϑ e W sono legate infatti con $\beta = v/c$ attraverso le relazioni:

$$\cos\vartheta = 1/\beta n \; ; \tag{1}$$

$$W = \frac{e^2 l}{c^2} \int_{\beta n > 1} \omega \, \mathrm{d}\omega \left(1 - \frac{1}{\beta^2 n^2}\right). \tag{2}$$

ove ω è la frequenza della luce).

Finora sono state eseguite soltanto determinazioni del primo tipo su fasci di molte particelle ben collimate, una determinazione di questo genere su una particella singola (come si richiederebbe nel caso dei raggi cosmici) appare molto difficile per ragioni di intensità, data la necessità di limitare l'angolo solido d'ingresso.

Con questa nota mi propongo di dimostrare la possibilità di impiego del secondo procedimento e di precisarne le condizioni. Il lavoro consta effettivamente di due parti: anzitutto occorreva accertare la possibilità di osservare la radiazione di Cerenkov con i mezzi a disposizione, poi determinarne l'energia.

Per il primo problema si è usato il dispositivo di fig. 1-*A*: un tubo metallico argentato all'interno, pieno d'acqua, ha la sezione meridiana calcolata in modo da concentrare la luce, emessa da particelle di $\beta = 1$ dirette secondo l'asse, in una regione anulare, una porzione della quale è occupata dal catodo di un fotomoltiplicatore 931A. Il raccordo in plexi-

(1) P. A. Cerenkov: *C. R. Acad. Sci. USSR*, **8**, 451 (1934).

(2) I. Frank e I. Tamm: *C. R. Acad. Sci. USSR*, **14**, 105 (1937).

(3) I. A. Getting: *Phys. Rev.*, **71**, 123 (1947).

(4) R. H. Dicke: *Phys. Rev.*, **71**, 737 (1947).

(5) J. V. Jelley: *Proc. Phys. Soc.*, A **64**, 82 (1951).

glas fra tubo e fotomoltiplicatore contribuisce a ridurre le perdite di luce per riflessione.

Il dispositivo potrà esser completato in seguito con l'aggiunta di un secondo

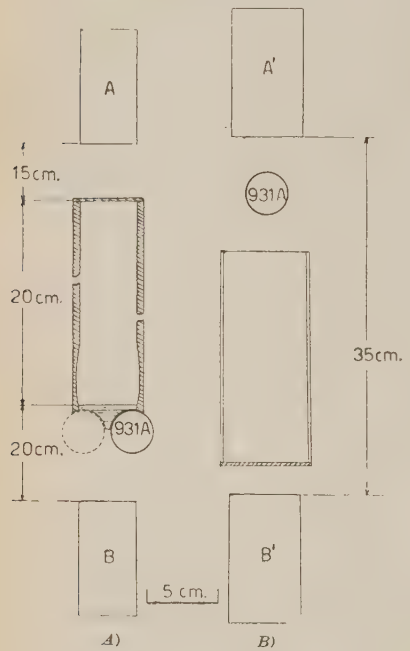

Fig. 1.

fotomoltiplicatore simmetrico al primo e in coincidenza con esso, e servire come contatore rapido di particelle cariche a velocità elevata. Il fotomoltiplicatore, a temperatura ambiente, comanda un preamplificatore ed un amplificatore di guadagno complessivo 10000 e tempo di salita $2 \cdot 10^{-7}$ s; gli impulsi amplificati sono fatti coincidere con quelli dei contatori AB. Abbiamo misurato le coincidenze triple col dispositivo dritto e capocapovolto ottenendo rispettivamente $1{,}53 \pm 0{,}17$ e $0{,}04 \pm 0{,}03$ coin/h (intensità calcolata 1,7 all'ora) in una delle molte serie di misure eseguite, tutte concordi. Se il fenomeno luminoso che osserviamo fosse dovuto a ordinarie scintillazioni di fluorescenza, non dovrebbe esserci questa asimmetria di rendimento: possiamo dunque asserire che si tratta di luce emessa per effetto Cerenkov.

Per il secondo problema, il dispositivo usato è quello di fig. 1-B: nell'angolo solido individuato dai contatori $A'B'$ è un recipiente cilindrico di vetro pieno d'acqua, con le pareti argentate ed il fondo ricoperto da uno strato di ossido di magnesio. Il fotomoltiplicatore 931A riceve raggi diffusi dal fondo, i cui contributi sono perciò indipendenti, almeno in prima approssimazione, sia dalla direzione di arrivo della particella che dall'angolo di emissione; il percorso della particella nell'acqua, poi, non varia in modo sensibile, nei limiti di precisione che ci siamo imposti, entro l'angolo solido definito dal telescopio dei contatori.

Gli impulsi del fotomoltiplicatore, dopo la solita amplificazione, entrano in un selettore di ampiezza a otto canali di tipo integrale e poi vanno a coincidere con gli impulsi dei contatori. Abbiamo ottenuto le curve di fig. 2 come differenza dei risultati di due misure, una con l'acqua, l'altra senza: la curva I si riferisce a una tensione applicata al foto-

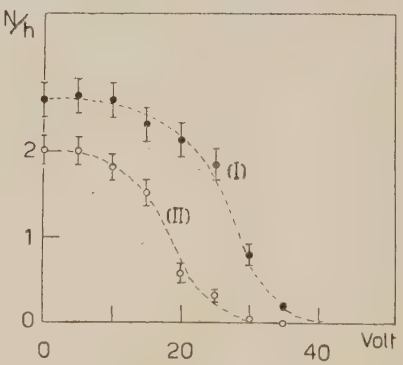

Fig. 2.

moltiplicatore di 85 volt per stadio, la curva II a 75 volt per stadio. Poichè il numero (calcolato) di raggi cosmici che attraversa il dispositivo è 10 all'ora, risulta, nel caso ad esempio di fig. 2(I)

un rendimento che si aggira sul 25 %. In queste condizioni è assai probabile che ogni raggio registrato produca un solo fotoelettrone. Alla stessa conclusione si giunge direttamente confrontando l'altezza più probabile dell'impulso proveniente dal fotomoltiplicatore con l'amplificazione complessiva del sistema fotomoltiplicatore-amplificatore.

I fotoni emessi, calcolati secondo la teoria di Frank e Tamm, nelle bande di frequenza utili, sono in media 3000 nel nostro dispositivo, ammettendo che i raggi cosmici abbiano tutti $\beta = 1$; da considerazioni geometriche si ricava che di questi soltanto qualche decina cadono sul fotocatodo: ne consegue che occorrono almeno 100 fotoni per produrre un fotoelettrone. Dalle curve differenziali che si deducono dalle integrali di fig. 2 (le quali si riferiscono, come abbiamo detto, ad un solo fotoelettrone) risulta che le deviazioni quadratiche medie relative introdotte dal sistema fotomoltiplicatore-amplificatore sono dell'ordine di 0,1. Questo risultato, in buon accordo con quello ottenuto da R. C. Hoyt [6] permette di affermare, seguendo un ragionamento analogo, che, quando i fotoelettroni siano qualche decina, il contributo dato alle fluttuazioni dal sistema fotomoltiplicatore-amplificatore, sarà trascurabile.

Tenendo conto del rendimento per i fotoni determinato prima e di queste considerazioni sugli scarti, risulta che, per valutare β per particelle singole occorre che sul fotocatodo giungano, ogni volta, almeno alcune migliaia di fotoni della radiazione di Cerenkov.

È in preparazione un dispositivo che dovrebbe funzionare in queste condizioni.

Ringrazio vivamente la dott. A. M. Bianchi che ha collaborato alle misure.

[6] R. C. Hoyt: *Rev. Scient. Inst.*, **20**, 178 (1949).

LIBRI RICEVUTI E RECENSIONI

F. SCHWANK: *Randwertprobleme.* VI + 406 pagg. B. G. Teubner Verlagsgesellschaft, Leipzig, 1951.

Gli argomenti contenuti in questo libro di SCHWANK (funzioni di variabile complessa, equazioni alle derivate parziali, equazioni integrali, calcolo delle variazioni, equazioni alle differenze finite) sono talmente classici e sono stati tante volte trattati nella letteratura scientifica, in quella tedesca in particolare, che si potrebbe a prima vista giudicarne del tutto pleonastica una nuova esposizione. Ciò nonostante la trattazione dei vari problemi e l'intento che l'autore si prefigge sono in complesso abbastanza originali da giustificare una nuova esposizione.

La differenza fra questo libro ed altri ben noti trattati dedicati allo studio delle stesse questioni (si pensi per esempio a quello celeberrimo di COURANT-HILBERT) sta nel fatto che il libro di SCHWANK non vuole essere un trattato ma semplicemente un'introduzione ad uso dei fisici e degli ingegneri, ai metodi della fisica-matematica: si tratta di un Lehrbuch e non di un Handbuch come osserva HAMEL nella prefazione al volume. Il principiante, e più ancora chi è obbligato ad approfondire le proprie conoscenze degli algoritmi matematici più elevati per risolvere i problemi presentati dalla fisica e dalla tecnica, prova sovente una notevole difficoltà nell'abbordare i trattati più completi di cui è ricca la letteratura fisico-matematica. Chi tale difficoltà ha provato accoglierà probabilmente con favore questo libro di SCHWANK, dove, se pure non potrà trovare una trattazione completa di tutti gli argomenti contenuti, potrà vedere quasi sempre un'impostazione sufficientemente chiara delle varie questioni e soprattutto potrà rendersi conto della connessione che esiste fra la matematica e il problema fisico.

Particolarmente utili sono i numerosi esercizi che illustrano i vari metodi esposti e che servono ottimamente a rendere proficuo il libro al lettore interessato all'aspetto applicativo e non puramente matematico e logico delle questioni. Anche gli esempi di applicazione degli strumenti matematici illustrati alla risoluzione dei problemi della fisica e specialmente della tecnica (in particolare nei capitoli dedicati alle equazioni integrali, al calcolo delle variazioni e alle equazioni alle differenze finite) risulta molto utile anche perchè essi sono completati da numerosi riferimenti bibliografici — magari un po' troppo parziali verso la letteratura tedesca e alquanto incompleti per quanto riguarda quella anglosassone più recente — a trattati e a memorie originali.

Naturalmente non mancano le questioni sulle quali si potrebbe dissentire con l'autore. È dubbio per esempio che la succinta esposizione del metodo di integrazione nel campo complesso, anche completata con l'esempio dato, possa riuscire effettivamente utile a chi desidera di impadronirsi di questo efficacissimo strumento matematico. A proposito della trattazione delle equazioni alle derivate parziali si può osservare che la mancanza di distinzione fra i vari tipi in base alle caratteristiche, ingenera una certa confusione e la mancanza della visione generale del problema.

Nonostante questi appunti ed altri che si potrebbero fare, il libro di SCHWANK può in complesso considerarsi come un utile contributo alla divulgazione dei metodi più elevati della fisica-matematica per i fisici e gli ingegneri.

L. A. RADICATI

Direttore responsabile: G. POLVANI

Tipografia Compositori - Bologna

Questo fascicolo è stato licenziato dai torchi il 23-IX-1951